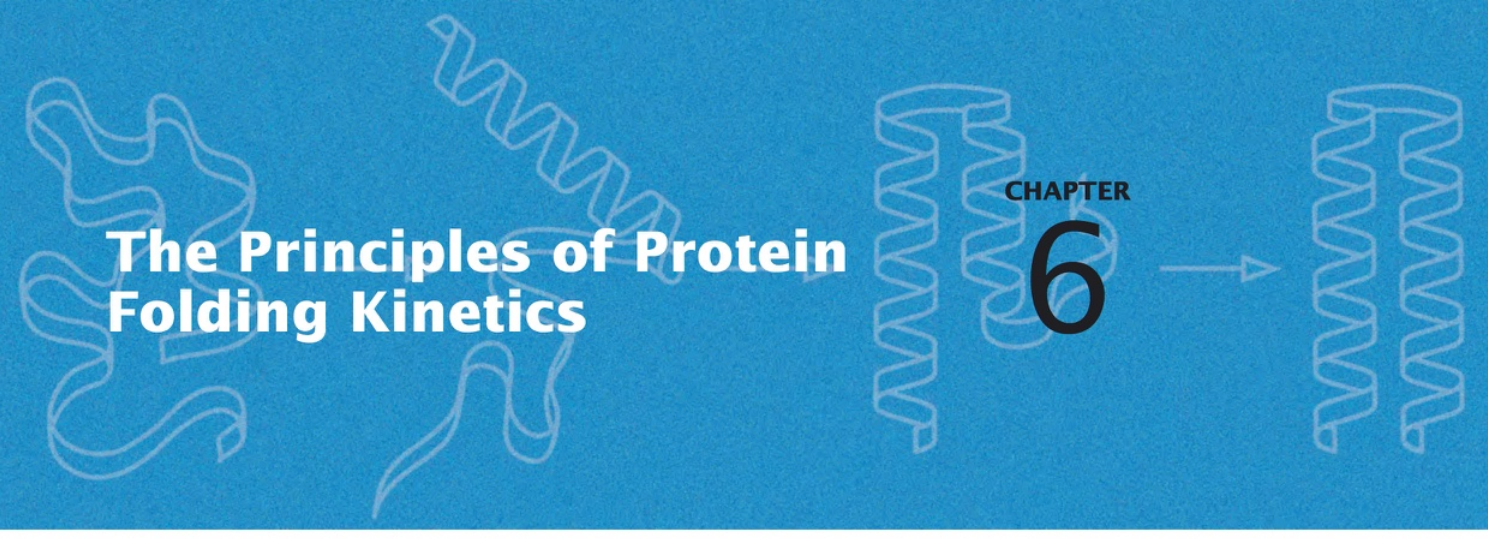

CHAPTER

6

The Principles of Protein Folding Kinetics

THE LEVINTHAL PARADOX MOTIVATED THE SEARCH FOR A PROTEIN FOLDING MECHANISM

In this chapter, we describe the rates and routes of protein folding and unfolding. By *routes*, we mean the time-course of conformational changes that occur as a protein folds. At what stage during the course of the folding process does a protein acquire its secondary structures, its hydrogen bonds, its hydrophobic core, and its tight side-chain packing? Is there a general mechanism that explains commonalities of folding and unfolding routes over different sequences and folds, and as a function of external variables, such as temperature and denaturants? How can a protein "find" its native structure spontaneously and quickly from its unfolded state, sometimes within microseconds? What is the *speed limit* of folding, and what is the physical basis for it?

Why is protein folding kinetics important? For one thing, folding kinetics was central to the historical development of protein science. In 1968, Cyrus Levinthal posed a puzzle that is called the "Levinthal paradox" [1]. Proteins face a "needle-in-a-haystack" problem. The haystack is the astronomically large conformational space that an unfolded protein must search in order to find the needle, its one native structure. If you estimate that there are between $z = 3$ and 8 conformational states for each peptide unit and if there are $N = 100$ amino acids in a protein, then the number of conformations the protein must search (the size of the haystack) is huge, $z^N \approx 10^{50}$–10^{90}. The Levinthal paradox is the question of how a protein can fold to its native structure so quickly, often in microseconds to seconds, in light of this huge search problem.

Levinthal's paradox inspired the following idea: if we could learn the *pathways* of folding, then perhaps we could infer a folding *principle* or *mechanism* by which conformations are explored or ignored, as so many different types of proteins reach their native structures so quickly and directly. Perhaps knowledge of the folding *intermediate states* (partially assembled structures that are formed on the way to the native state) could give us clues about how each type of protein "knows" which vast stretches of its conformational space not to search. Such

knowledge could help us improve computer search methods for predicting native protein structures from their amino acid sequences. And knowledge of folding kinetics could help us understand the dynamics of other processes, including ligand binding, allosteric changes in conformation, and mechanistic actions.

FOLDING RATE EXPERIMENTS ARE CAPTURED BY MASS-ACTION MODELS

We begin with the most basic experiment in folding kinetics. You start with a dilute solution of proteins that are unfolded because of the denaturing conditions of the solution. You switch the solution to *folding conditions* by suddenly changing the denaturant concentration, pH, or temperature. You then observe an optical property, such as circular dichroism (CD) or fluorescence, $y(t)$, as a function of time t. You monitor the rate of the increasing population of native molecules in the test tube. This type of experiment is often called *in vitro refolding*, because it takes place in test tubes, not inside the cell, with proteins that were initially unfolded. You can also run the experiment in reverse, unfolding native proteins by jumping the protein solution from native conditions to *unfolded conditions*. You run these experiments with dilute protein solutions, to avoid protein aggregation.

Folding and unfolding processes are usually well described by one or more exponential functions of time:

$$y(t) = A_1 e^{-k_1 t} + A_2 e^{-k_2 t} \tag{6.1}$$

(Figure 6.1). The rate coefficients k_1 and k_2 and the amplitudes A_1 and A_2 can give you insights into the folding process under various conditions.

In this chapter, we describe the insights you get from both *macroscopic* and *microscopic* models. In macroscopic modeling, your goal is

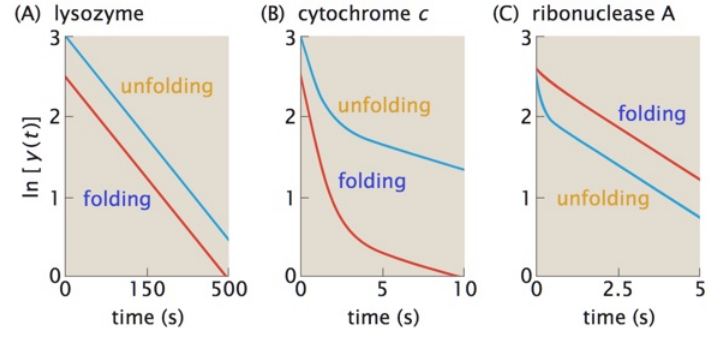

Figure 6.1 Folding and unfolding often follow one- or two-exponential decays. Kinetic relaxation of the amount of native or denatured protein as a function of time after jumping the conditions by light absorbance for (A) lysozyme and (B) cytochrome *c*, and by fluorescence for (C) ribonuclease A. A single exponential is a straight line on these logarithmic plots. The plots show two-state folding and unfolding kinetics for lysozyme; three-state folding and unfolding for cytochrome *c*; and a combination of two-state folding and sequential unfolding for ribonuclease A. (A and B, adapted from A Ikai and C Tanford. *Nature*, 230:100–102, 1971. With permission from Macmillan Publishers Ltd.; C, adapted from TY Tsong, RL Baldwin, and EL Elson. *Proc. Natl Acad Sci USA*, 69:1809–1812, 1972. Copyright (1972) National Academy of Sciences, USA.)

to choose the *mass-action model* that best fits your data. A *mass-action model* is a chosen set of *kinetic states*, such as D, I, and N, and a postulated kinetic scheme of arrows connecting those states (Figure 6.2). Macroscopic modeling simply expresses your experimental results in the shorthand language of these *pathways*. In contrast, microscopic models aim to capture the underlying physics—how the molecular conformations and energies lead to folding rates and routes. Microscopic models aim to give a structural and physical explanation for the time evolution of folding events, and/or the effects of temperature, denaturants, pH, or amino acid sequence on the folding process. First, let's explore macroscopic modeling.

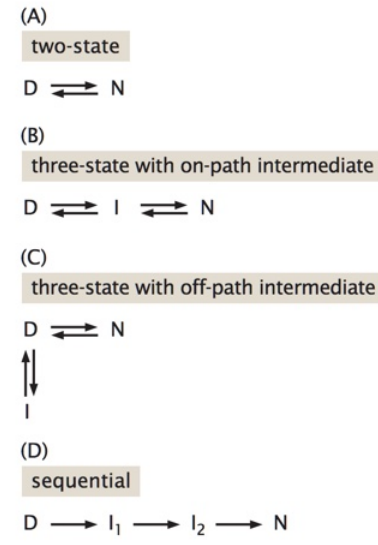

Figure 6.2 Common mass-action models of folding. (A) The two-state model. (B) On-pathway intermediate state. (C) Off-pathway intermediate. (D) A sequential model having multiple intermediates.

Small Proteins Fold Rapidly through Two-State Kinetics

A typical small single-domain protein folds or unfolds in just a single-exponential relaxation process, such as the one shown in Figure 6.1A for lysozyme. Processes in nature that involve single-exponential dynamics are said to follow *two-state* kinetics because the mass-action model you need to explain them requires only two states, in this case D (denatured) and N (native):

$$\mathrm{D} \underset{k_u}{\overset{k_f}{\rightleftharpoons}} \mathrm{N}, \tag{6.2}$$

where k_f and k_u are the folding and unfolding *rate coefficients*,[1] respectively. The time dependence of this process can be described by

$$\begin{aligned} \frac{d[\mathrm{D}]}{dt} &= -k_f[\mathrm{D}] + k_u[\mathrm{N}], \\ \frac{d[\mathrm{N}]}{dt} &= k_f[\mathrm{D}] - k_u[\mathrm{N}], \end{aligned} \tag{6.3}$$

where [D] and [N] are the time-dependent concentrations of the denatured and native states, respectively. If you choose normalized units so that $[\mathrm{D}] + [\mathrm{N}] = 1$, then [D] and [N] are time-dependent *probabilities* or *populations*, $p_\mathrm{D}(t)$ and $p_\mathrm{N}(t)$, with values ranging from 0 to 1.

There are different ways to solve Equation 6.3. The simplest is to substitute $p_\mathrm{D}(t) = 1 - p_\mathrm{N}(t)$ and solve for $p_\mathrm{N}(t)$. However, that strategy is limited mostly to two-state kinetics. Because we want to explore a broader range of models that apply to different types of dynamics, we use a more general approach, called *master equations*. In this approach, you express the probabilities of the states in a *column vector*

$$\mathbf{P}(t) = \begin{bmatrix} p_\mathrm{D}(t) \\ p_\mathrm{N}(t) \end{bmatrix} \tag{6.4}$$

and the rate coefficients in a *rate matrix*

$$\mathbf{W} = \begin{bmatrix} -k_f & k_u \\ k_f & -k_u \end{bmatrix}. \tag{6.5}$$

[1] We use the term *rate coefficient* rather than *rate constant*, which is common in the field, because these quantities are not constants. They are usually strong functions of temperature, among other things.

Then, you can express the time evolution of the probabilities as a matrix equation:

$$\frac{d\mathbf{P}(t)}{dt} = \mathbf{W}\mathbf{P}(t). \tag{6.6}$$

Appendix 6A gives the procedure for solving master equations. For the earlier two-state case, the native population is

$$p_{\mathrm{N}}(t) = p_{\mathrm{N}}(0)e^{-(k_u+k_f)t} + \frac{k_f}{k_u+k_f}\left(1 - e^{-(k_u+k_f)t}\right), \tag{6.7}$$

and the denatured population is $p_{\mathrm{D}}(t) = 1 - p_{\mathrm{N}}(t)$. The fraction of molecules that are folded converges to the equilibrium value

$$p_{\mathrm{N}}(\infty) = \frac{k_f}{k_f + k_u} \tag{6.8}$$

at long times. Equation 6.7 says that if you jump the conditions at time $t = 0$, you will observe a single-exponential decay to equilibrium with a rate coefficient

$$k_{\mathrm{obs}} = k_u + k_f. \tag{6.9}$$

In one limit, you can start at time $t = 0$ with all molecules unfolded, $p_{\mathrm{N}}(0) = 0$, and apply strong folding conditions, $k_u \to 0$. Then the native-state population will grow exponentially with time, with rate coefficient k_f:

$$p_{\mathrm{N}}(t) = 1 - e^{-k_f t}. \tag{6.10}$$

In the opposite limit, you can start at time $t = 0$ with all molecules fully folded, $p_{\mathrm{N}}(0) = 1$, and apply strong denaturing conditions, $k_f \to 0$. Then the native-state population will disappear exponentially:

$$p_{\mathrm{N}}(t) = e^{-k_u t}. \tag{6.11}$$

Here is how you use Equation 6.7. You adjust the parameters k_f and k_u to achieve the best fit of Equation 6.7 to your experimental data. If your data are more complex than single-exponential dynamics, then you try a different model, typically one that has intermediate states.

The two-state dynamics described earlier is often adequate for small proteins. How should you interpret this exponential time dependence? Does it mean that all the proteins in the test tube are synchronized, with each molecule forming its first helix at the same time that every other protein molecule forms its first helix, for example? Or does it mean that each protein itself folds very quickly, not synchronized with other protein molecules, and that the exponential decay is just reflecting what fraction of the protein molecules are folded or unfolded at a given time? It means the latter. The rate coefficients k_f and k_u are the probabilities per unit time that any particular protein molecule will convert. The *number of molecules* that convert to N at any given time is proportional to how many D molecules are still left unconverted in the test tube at that time. The fewer D molecules there are in solution, the fewer D $\to$ N conversions happen in unit time. This is a concentration effect. This is the basis for the exponential time course in protein folding or unfolding. Box 6.1 shows how you can use this interpretation for determining folding rates from computer simulations.

Box 6.1 You Can Estimate a Protein's Folding Rate from Multiple Short Computer Simulations

Suppose you want to run a computer simulation of folding to determine the folding rate coefficient k_f. (Such simulations are discussed in Chapter 10.) You can run either a few long trajectories or many short ones. You could start the simulation from some unfolded conformation, then run a long trajectory of the protein under folding conditions. Your computer trajectory should be run for at least several multiples of the time $\tau_f = 1/k_f$, the inverse of the folding rate coefficient. Otherwise, you won't have enough data to accurately fit the baseline of your relaxation curves. For example, if the true folding time were 1 μs, you would need at least 5–10 μs of simulation time. But running long trajectories takes a long time on computers.

Instead, if you have parallel computers, you could run many short trajectories and collect statistics. V Pande showed this on a computer resource called Folding@home. Equation 6.10 shows that for short times ($t \ll \tau_f$), starting from the denatured state, you can approximate the time-dependent population of the native state as

$$p_N(t) = 1 - e^{-k_f t} \approx k_f t. \tag{6.12}$$

Rearranging Equation 6.12 gives

$$k_f = \frac{p_N(t)}{t} \tag{6.13}$$
$$= \frac{1}{t}\left(\frac{\text{number of trajectories in which the protein folds}}{\text{total number of trajectories}}\right).$$

In this way, you can estimate k_f from many short trajectories instead of fewer long ones. You simply count the fraction of folding events you see. This strategy is useful because it is often easier to obtain computer resources for many shorter runs than for fewer long ones. And long trajectories do not necessarily provide adequate sampling of conformational space.

Small globular proteins (shorter than about 100–150 amino acids) usually fold via two-state kinetics. It is remarkable that proteins fold with such simple kinetics, given their heterogeneous and complex molecular structures. We show in the following that any process having single-exponential kinetics can be described as having a *rate-limiting step*, or a *transition state*.

Single-Exponential Kinetics Is Characterized through the Concept of a *Transition State*

Any process having single-exponential dynamics, including two-state protein folding or unfolding, can be described using a concept called *transition state* or *activation barrier*. This concept rests on the fundamental relationship between any equilibrium constant K, such as for folding, and its corresponding free-energy change ΔG_f:

$$\Delta G_f = G_N - G_D = -RT \ln K, \tag{6.14}$$

where RT is the gas constant multiplied by the absolute temperature, and G_N and G_D are the free energies of the native and denatured states, respectively. For two-state kinetics, you can express the equilibrium constant as a ratio of rate coefficients:

$$K = \frac{[N]_{eq}}{[D]_{eq}} = \frac{k_f}{k_u}. \tag{6.15}$$

The first equality is the definition of the equilibrium constant for a two-state process, and the second comes from using equilibrium condition $d[N]/dt = d[D]/dt = 0$ in Equation 6.3.

From substituting Equation 6.15 into Equation 6.14, it follows that

$$\begin{aligned} \Delta G_f &= -RT \ln\left(\frac{k_f}{k_0}\right) - \left[-RT \ln\left(\frac{k_u}{k_0}\right)\right] \\ &= \Delta G_f^{\ddagger} - \Delta G_u^{\ddagger}. \end{aligned} \tag{6.16}$$

Equation 6.16 simply relates rate coefficients to free-energy quantities, just as Equation 6.14 expresses *equilibria* in terms of free energies. (We have introduced an *intrinsic rate* constant k_0 into each term on the right-hand side. Mathematically, k_0 is needed to ensure that each argument inside each logarithm is dimensionless. Physically, k_0 represents the maximum speed that either forward or reverse processes can reach, at infinite temperature.) Following immediately from Equation 6.16 is the existence of a third state, represented by ‡, that is neither N nor D, and that has free energy $G^{\ddagger}$:

$$\Delta G_f^{\ddagger} = -RT \ln\left(\frac{k_f}{k_0}\right) = G^{\ddagger} - G_D \tag{6.17}$$

and

$$\Delta G_u^{\ddagger} = -RT \ln\left(\frac{k_u}{k_0}\right) = G^{\ddagger} - G_N. \tag{6.18}$$

The state ‡ is called the *transition state* (TS) or *activated state*, and $G^{\ddagger}$ is its free energy. Rearranging Equation 6.17 gives the folding rate coefficient in terms of the barrier free energy:

$$k_f(T) = k_0 \exp\left(-\frac{\Delta G_f^{\ddagger}}{RT}\right). \tag{6.19}$$

The state ‡ can be regarded as a bottleneck; it usually has a positive free energy, $\Delta G_f^{\ddagger} > 0$, meaning that both the forward and backward rates of the system are slower than the speed limit, that is, $k_f/k_0 < 1$ and $k_u/k_0 < 1$. So, $G^{\ddagger}$ represents a hilltop point on a *reaction-coordinate diagram* (Figure 6.3). A reaction diagram is a plot of the free energies of the various states along the way between the two end states. Reaction-coordinate diagrams convey the information that the forward and reverse rates can be expressed in terms of free energies, and that there is a sum relationship between the free energies: $\Delta G_f = \Delta G_f^{\ddagger} - \Delta G_u^{\ddagger}$. Any process involving single-exponential kinetics is interpretable in terms of transition-state barriers. The importance of Equation 6.19 is in describing an experimentally observable quantity, the folding rate coefficient, in terms of another quantity, the free-energy barrier, that expresses underlying driving forces.

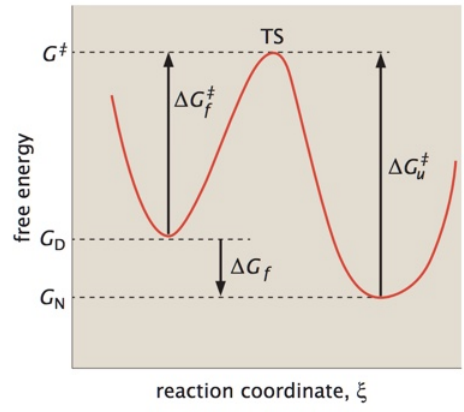

Figure 6.3 A reaction-coordinate diagram is a one-dimensional representation of the relationship between equilibrium and rate quantities: $\Delta G_f = \Delta G_f^\ddagger - \Delta G_u^\ddagger$. This diagram conveys this relationship on a diagram showing a real or fictitious *reaction coordinate* ξ, which represents the progress of the reaction.

Here's how the transition-state concept is used for proteins. First, it implies a possible structural basis for rate bottlenecks. Is there a particularly "challenging" structure of the protein that causes it to be the slow step in folding? However, protein folding is different than small-molecule chemistry, where the transition-state concept is traditionally applied. The making and breaking of covalent chemical bonds involves large energies, usually tens of kilocalories per mole, whereas the making and breaking of noncovalent bonds, as in protein folding, involves much smaller energies, in the range of $RT = 0.6\,\text{kcal mol}^{-1}$ at $T = 300\,\text{K}$. So, transition states for protein conformations are *thermal ensembles*, not single molecular structures.

Second, the transition-state equation, Equation 6.19, is also useful for interpreting the effects of temperature on kinetics. If you observe that $\ln k_f(T)$ is proportional to $1/T$, it implies that k_0 and $\Delta G_f^\ddagger$ are constants, independent of temperature. In this case, called *Arrhenius kinetics*, increasing the temperature increases the speed of a process. Arrhenius kinetics is often observed for protein *unfolding* and for conformational changes of small protein pieces, such as helices and β-hairpins. However, Arrhenius kinetics are sometimes not observed for protein *folding*: for ultrafast-folders, heating doesn't speed up folding. We give examples later in this chapter.

What is the speed limit k_0? The speed limit of gas-phase chemical reactions is $k_0 = RT/h = 0.16$ conversions per picosecond at room temperature (h is Planck's constant). But protein-folding kinetics is not comparable to that of chemical-bond-forming reactions in the gas phase. Folding entails a protein sloshing around in solvent. The shortest time for protein folding has been estimated to be around 1 μs, so for protein folding, $k_0 \approx 10^6\,\text{s}^{-1}$ [2]. This also happens to be approximately the maximum speed that a 10- or 20-mer peptide can form a helix in solution.

Large Proteins Typically Fold via Multi-Exponential Kinetics

Large proteins tend to fold slowly, and with multi-exponential rates. By definition, the two-state model will not fit a multi-exponential process. To fit two exponentials, you must invoke at least three states, typically native, denatured, and a *kinetic intermediate* state. There are two main types of three-state models. In the model $\text{D} \rightleftharpoons \text{I} \rightleftharpoons \text{N}$, the folding intermediate state I is called *on-pathway* because the symbol

appears in-line between D and N. On the other hand, if your data may be better fit by the model, $I \rightleftharpoons D \rightleftharpoons N$, then the intermediate state I is called *off-pathway*, or is sometimes referred to as a *misfolded intermediate*, because it is not directly in-line between D and N. You choose between on-path and off-path models (and possibly other models) based on whichever model gives the best fit to the data. And, when neither on-pathway or off-pathway models fits, then try a different model. For example, the folding of ribonuclease A (see Figure 6.1C) has been explained [3] by a sequential, four-state model, similar to the one shown in Figure 6.2D.

What Is the Difference between a Kinetic Intermediate State and a Transition State?

The expression $D \rightarrow TS \rightarrow N$ resembles the expression $D \rightarrow I \rightarrow N$. What is the difference between a kinetic intermediate state I and a transition state TS? Intermediates are defined as states that become substantially populated during a kinetic process, while transition states do not. Think of the kinetic states D, N, or the intermediates, $I_1, I_2, \ldots I_m$, as metaphorical "buckets" that can fill up and empty out. In this metaphor, the folding process begins with a full bucket D and an empty bucket N. Folding ends when the N bucket is full and D is empty. Now consider a situation in which there is an intermediate bucket (labeled either I or TS) interposed between D and N. Bucket D pours into this intervening bucket, which has a hole in its bottom, so it empties into bucket N. The difference between an intermediate and a transition state is the size of the hole in the middle bucket. As the D bucket pours into an intermediate I, the I bucket leaks out into the N bucket only slowly, so the I bucket fills up significantly throughout the middle of the kinetic process, before it drains out at later times. In contrast, think of TS as a bucket that has a large hole in its bottom, so that it never fills up very much (Figure 6.4A). Even if the D bucket is pouring into the TS bucket rapidly, the TS bucket empties into the N bucket as fast as it is being filled, so TS never becomes very full. In short, I states reach significant populations and observable kinetic features, while TS states have only small populations, so they are consistent with only two observable kinetic states.

Our buckets are simply a metaphor for the *eigenvectors* of a master equation; see Appendix 6A. Once you know the dynamics of a model, you can compute its eigenvalues and eigenvectors. Think of one eigenvalue (a rate) and an eigenvector (a set of changes in the populations of states reflecting the inflows and outflows of the different states)

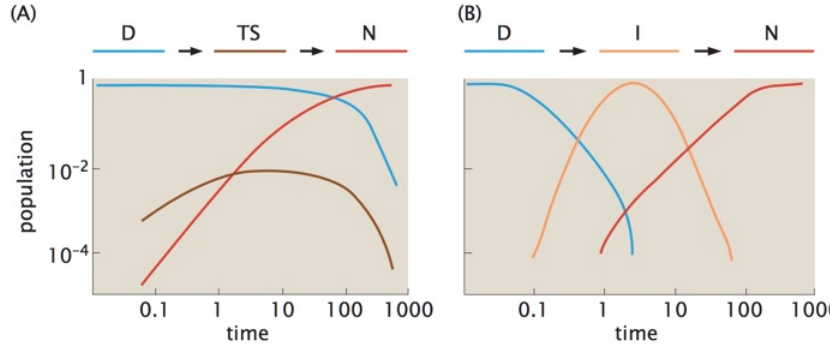

Figure 6.4 Transition states have small populations. Kinetic intermediates have larger populations. The plots show populations of states versus time since the initiation of folding. (A) The transition state (TS) in $D \rightarrow TS \rightarrow N$ is only transient, never reaching a high population, and not contributing an observable kinetic phase. (B) The intermediate state (I) in $D \rightarrow I \rightarrow N$ has a detectable population during the folding process, leading to an observable kinetic phase (see [4]).

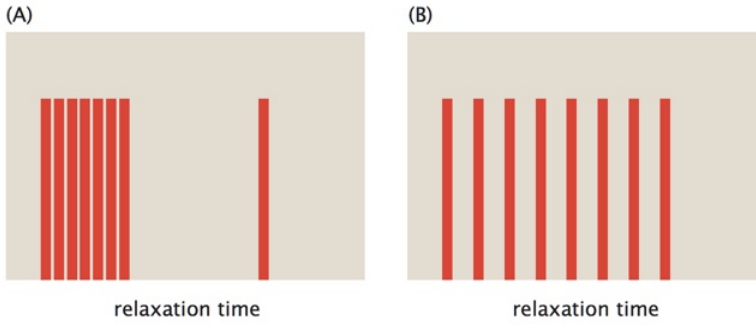

Figure 6.5 A gap in the eigenvalue spectrum implies apparent two-state kinetics. The bars indicate the different relaxation times of multi-exponential processes. Different processes have characteristic spacings. (A) When the eigenvalue spectrum has a single slowest process that is well separated from other (faster) processes, the slowest exponential will be the most prominent observable, since faster processes will equilibrate over that timescale. (B) When the eigenvalues are not well separated, the kinetics are more complicated and multi-exponential.

as describing one "generalized process" or metaphorical "generalized bucket". Solving a master equation gives a sum of such generalized independent processes. Each process has its own timescale (eigenvalue). Each process is a sum of different amounts of flows to and from the different states. Eigenvalues and eigenvectors are the quantitative manifestation of the bucket idea. They express a given relaxation process as a sum of contributions from different modes of relaxation. Each reaction *topology* (that is, particular arrangement of states and arrows) leads to some eigenvalue spectrum. Single-exponential kinetics is observed when an eigenvalue spectrum has a gap between the slowest rate and all others (Figure 6.5A). In multi-exponential kinetics, there is no such gap between eigenvalues (see Figure 6.5B).

RATE MEASUREMENTS GIVE INSIGHTS INTO THE PATHWAYS OF PROTEIN FOLDING

What are the folding *routes*? When do different structures form during the folding process? Different experimental probes will report different information. Suppose you have two probes, one that reports helix formation and another that reports chain collapse. In principle, watching the time dependence of both probes during a folding experiment of a protein could tell you the relative order of the collapse and helix-formation events of that protein. But here's the challenge. The small proteins that are commonly studied are two-state folders; that is, they fold with only a single kinetic phase. So, without other information, all you can say about two-state folders is that "everything happens within a single kinetic event." If you want to create a more detailed narrative about folding pathways, you need independent information or you need to study multistate folders, where you can characterize the kinetic intermediate states.

Figure 6.6 shows three hypothetical folding pathways. In one, folding happens as a single event. Another possibility is that two helices form separately at about the same time, and then the two fully formed helices dock together. A third option is that one helix forms first, providing a surface onto which the second helix can form. And, there are many other options. The search for folding mechanisms has driven

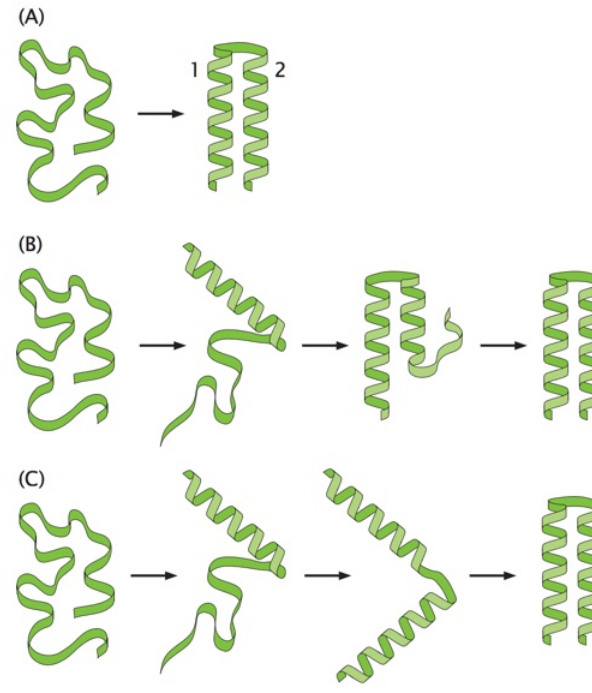

Figure 6.6 Different possible folding routes. Different kinetic routes from the denatured state (disordered, on the left) to the native state (helices, on the right). (A) Two-state process: it happens all at once. (B) First, helix 1 forms, which serves as a template, assisting the formation of helix 2. (C) Helix 1 forms independently of helix 2, then they come together.

important advances in experimental methods, some of which are described in this chapter.

One well-studied kinetic intermediate state involves *proline isomerization*. Prolines can interconvert between two different isomeric states, *cis* and *trans* peptide bonds. In the native structure, the proline interconversion is slow. In the denatured protein, the proline will be in a Boltzmann equilibrium between the two isomeric states. Upon folding, each of the protein's non-native prolines must convert to whatever is that proline's native-state isomer. So, folding has two kinetic phases. In the slow phase, the protein starts with the wrong proline isomer. That folding is slow because prolines are slow to isomerize. In the fast phase, the protein begins in conformations that are already in the correct isomeric state.

Another kinetic intermediate is found in the folding of the bovine pancreatic trypsin inhibitor protein (BPTI), whose native structure has three disulfide bonds among six Cys residues. Interestingly, the disulfide bonds in BPTI do not form in a systematic increasingly native-like series of events. Some wrong disulfide bonds form transiently first, then they are undone, then the correct disulfides finally form. These incorrect disulfides have been called *on-pathway misfolded states*.

Other proteins, too, can pass through non-native states on their folding routes. The folding kinetics of lysozyme shown in Figure 6.1A indicates a single exponential, when probed by a single method. However, by using multiple methods, it has been shown that the two domains of hen lysozyme behave differently during folding. The α-domain folds rapidly. Once the α-domain is formed, the β-domain then folds. The protein overshoots in the fast process, indicating that helix formation probably goes too far, and leads to non-native contacts, before being rescued by the slower β-sheet formation step. The folding of

hen lysozyme thus appears to involve multiple paths and considerable complexity [5]. β-lactoglobulin also folds with multiphase kinetics. β-lactoglobulin is a β-barrel comprised of nine antiparallel β-strands, one major α-helix, and four short helices. In folding, the molecule first forms an α-helical structure transiently before adopting its native β-barrel structure.

Mutational Studies Can Probe Folding Pathways

You can get insights into folding routes by studying mutated proteins. A method called Φ-*value analysis* [6] gives information about which parts of the protein fold slowly and which fold more rapidly. In Φ-value analysis, you mutate a single amino acid at a time in the protein. You measure both the folding rate coefficient $k_{f,\,\mathrm{wt}}$ of the wild-type protein and the folding rate coefficient $k_{f,\,\mathrm{mut}}$ of the mutant. Equation 6.17 indicates that the *change* in the transition-state barrier free energy resulting from the mutation will be given by

$$\Delta\Delta G_f^{\ddagger} = -RT \ln\left(\frac{k_{f,\,\mathrm{mut}}}{k_{f,\,\mathrm{wt}}}\right). \tag{6.20}$$

To perform Φ-value analysis, you must also measure the change in protein stability, $\Delta\Delta G_f$, caused by the mutation, or equivalently the change in equilibrium constant of the mutant, $K_{f,\mathrm{mut}}$, relative to that of the wild type, $K_{f,\mathrm{wt}}$. The Φ value for folding is defined as the ratio

$$\Phi_f = \frac{\Delta\Delta G_f^{\ddagger}}{\Delta\Delta G_f} = \frac{\ln(k_{f,\,\mathrm{mut}}/k_{f,\,\mathrm{wt}})}{\ln(K_{f,\,\mathrm{mut}}/K_{f,\,\mathrm{wt}})}. \tag{6.21}$$

Φ is a number that is usually between 0 and 1. Figure 6.7 shows how Φ values are interpreted in terms of transition states.[2] Observing $\Phi_f = 0$ means that your mutation had no effect on the folding rate. Observing $\Phi_f = 1$ means that your mutation affected the folding free-energy barrier as much as it affected the folding stability. So, mutational results

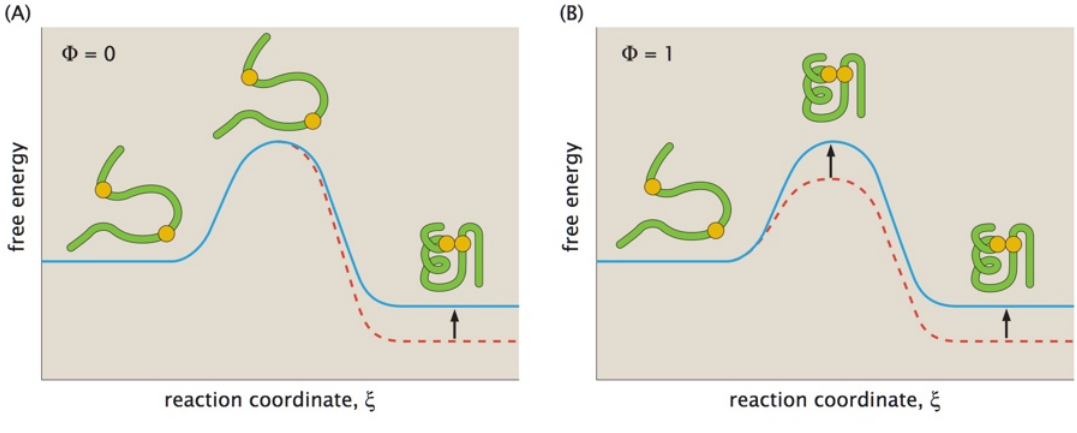

Figure 6.7 A Φ value is often interpreted in terms of a structure of the transition state. (A) Φ = 0 means that the mutation site has a denatured-like structure when it is in its transition state. (B) Φ = 1 means that the mutation site has a native-like structure when it is in its transition state. The *blue solid curve* is for wild type, and the *red dashed curve* is for mutant.

[2] We have described here the *folding* Φ value, Φ_f; you can also define a corresponding *unfolding* Φ_u.

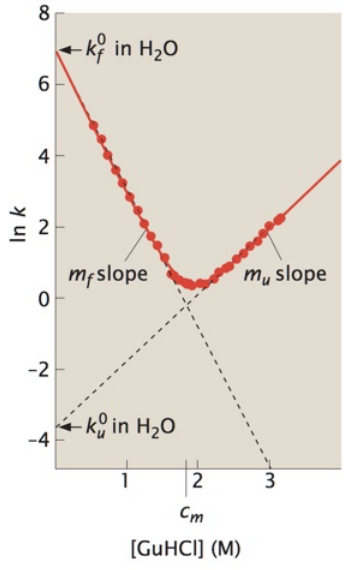

Figure 6.8 A chevron plot shows how denaturants affect folding kinetics. The *left straight* line shows that reducing the denaturant concentration speeds up folding. The *right straight* line shows that increasing denaturant speeds up unfolding. c_m is the denaturation midpoint. Extrapolation of the lines to zero denaturant gives the folding and unfolding rate coefficients k_f and k_u in water. The results shown here are for the acyl-CoA-binding protein. (Adapted from KL Maxwell, D Wildes, A Zarrine-Afsar, et al. *Protein Sci*, 14:602–616, 2005.)

are often interpreted as follows. If you see $\Phi_f = 0$ for your mutation, it means that residue in the chain has not yet reached its folded structure when the rest of the chain is passing through the transition state, while $\Phi_f = 1$ means that residue is native when the chain passes through its folding transition state.

If you find nonzero $\Phi > 0$ at multiple sites, then the transition state is called *diffuse*, meaning that many different amino acids in that protein are involved in controlling the folding rate. If, instead, you find $\Phi \approx 0$ broadly throughout the protein, the transition state is called *polarized*, meaning that just a few of the protein's amino acids are controlling the folding rate. For example, chymotrypsin inhibitor 2 has a diffuse transition state, and ubiquitin has a polarized transition state.

Denaturants Can Change Folding Rates: The Chevron Plot

Adding denaturants, such as guanidinium hydrochloride (GuHCl) or urea, can slow down folding and speed up unfolding. The effects of denaturants on folding rate coefficients are represented using a *chevron plot*. A chevron plot shows the logarithm of the observed relaxation rate on the vertical axis versus the denaturant concentration on the horizontal axis (Figure 6.8). The term *chevron* refers to the plot's V shape (or inverted-V shape if you plot the logarithm of folding time instead). The left branch of the V describes the folding rates you see when the system is jumped to low denaturant concentrations, telling you about the folding process. The right branch of the V describes jumping to high denaturant concentrations, telling you about the unfolding process.

For proteins that fold with two-state kinetics, the logarithm of folding and unfolding rate cooefficients are linear functions of denaturant concentration $[d]$ (see Figure 6.8); that is,

$$\begin{aligned} \ln k_f &= \ln k_f^0 + m_f[d], \\ \ln k_u &= \ln k_u^0 + m_u[d]. \end{aligned} \tag{6.22}$$

$m_f < 0$ and $m_u > 0$, which are called *kinetic m-values*, are the slopes of the two lines. Adding denaturant slows protein folding and speeds up protein unfolding. The linear behavior of the logarithm of *rate coefficients* with denaturant concentration in a chevron plot resembles the linearity of the logarithm of *equilibrium constants* (the *m*-values) for protein stabilities (see Chapter 3). k_f^0 and k_u^0 are the folding and unfolding rates, respectively, in the absence of denaturant. For proteins that obey two-state folding/unfolding kinetics, you can relate the equilibrium unfolding free energy $\Delta G_u = -\Delta G_f$ to the folding and unfolding rate coefficients:

$$\Delta G_u = RT \ln\left(\frac{k_u}{k_f}\right) = RT \ln\left(\frac{k_u^0}{k_f^0}\right) + (m_u - m_f)[d]. \tag{6.23}$$

At the denaturation midpoint (that is, at c_m in Figure 6.8), you have $k_f = k_u$.

Why are chevron plots V-shaped? Recall from Equation 6.9 that the observed relaxation rate coefficient is the sum of folding and unfolding

rate coefficients: $k_{obs} = k_f + k_u$. At low denaturant concentrations, the protein is native and k_u is small, so $k_{obs} \approx k_f$, and therefore the left arm reports mostly on the folding process. At high denaturant concentrations, the protein is denatured and k_f is small, so $k_{obs} \approx k_u$ (see Figure 6.8). Therefore, you get two straight lines when you plot the logarithm of k_{obs} versus denaturant concentration, giving a shape like the letter V. Kinetic m -values for several small proteins are given in Maxwell et al. [7].

A V-shaped plot indicates that a protein has two-state folding kinetics. When folding is more complex than a single exponential, a chevron plot is not V-shaped. Figure 6.9 shows *rollover*, where one arm of a chevron plot is curved or forms a plateau, rather than a straight line. Rollover indicates the presence of a folding intermediate or a kinetic trap: further strengthening the folding conditions (moving to the left on the *x*-axis of the chevron diagram) doesn't speed up folding. Rollover means that a stronger external driving force cannot overcome some internal speed limit of the protein.

You can combine mutations with chevron plots. To do this, you first measure the folding and unfolding rates of your protein in a series of different denaturants, to make a chevron plot for your wild-type protein. Then you make a mutation at a particular amino acid site in the protein. Now, you make another chevron plot for the mutant. Plot the two chevrons on the same figure. Figure 6.10 shows two limiting cases: (A) In one case, the mutation changes the folding arm of the chevron plot, but not the unfolding arm. This indicates the mutation site contributes to folding-rate control. (B) In the other case, the mutation changes the unfolding arm, but not the folding arm. This indicates the mutation site is not rate-controlling for folding.

Here is a key implication from chevron studies on two-state proteins: the main folding mechanism (the slowest step) is independent of the starting state of the protein. The folding arm of a chevron plot is determined fully by the final state of the solution to which the protein is jumped. The folding arm does not depend on the initial state of the protein prior to the jump in conditions. You could have started the folding process from highly denaturing conditions, where the protein would have no partially folded structure. Or you could have started the folding process from weakly denaturing conditions, where the protein might have had considerable partial structure. It doesn't matter. The slowest relaxation time doesn't change as a function of different initial conditions.

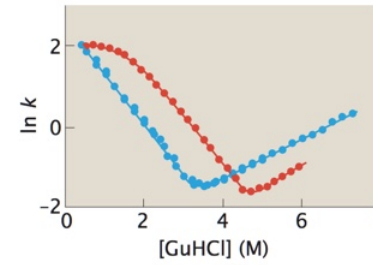

Figure 6.9 Adding salt speeds up folding and slows down unfolding. Chevron plots for the folding of ribosomal protein S6, in the absence (*blue*) and the presence (*red*) of sodium sulfate. The rollover (*red*) indicates that folding reaches maximum speed at low denaturant concentrations. The salt stabilizes the native protein. (Adapted from DE Otzen and M Oliveberg. *Proc Natl Acad Sci USA*, 96:11746–11751, 1999. Copyright (1999) National Academy of Sciences, USA.)

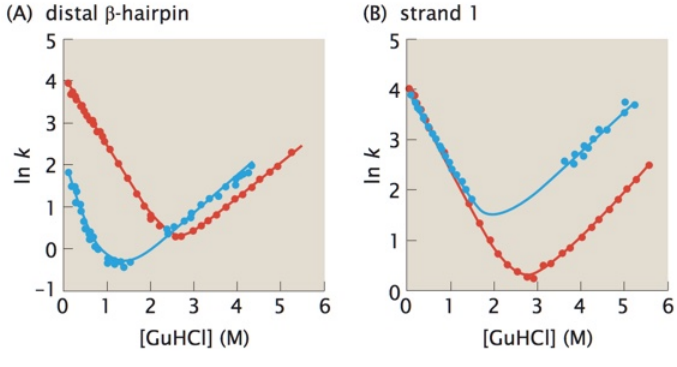

Figure 6.10 Some mutations change folding rates; some change unfolding rates. (A) Mutations in the "distal" β-hairpin of the SRC kinase SH3 domain change only the folding arm of the chevron plot. (B) Mutations in the first β-strand change only the unfolding arm. Wild type is shown by *red* and mutant by *blue*. (Adapted from DS Riddle, VP Grantcharova, JV Santiago, et al. *Nat Struct Biol*, 11:1016–1024, 1999. With permission from Macmillan Publishers Ltd.)

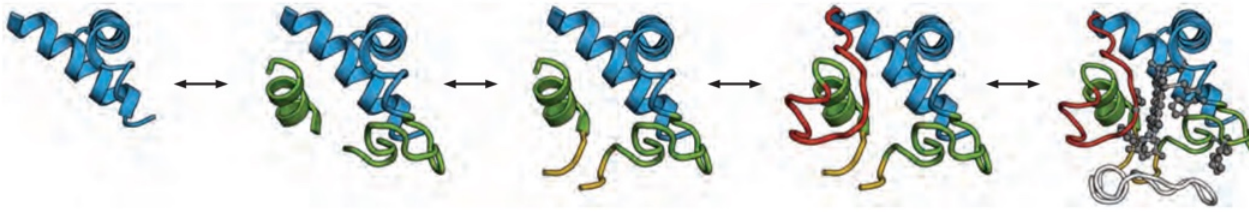

Figure 6.11 Cytochrome *c* folds in units of foldons. The foldon units are the pair of two terminal helices that form a tertiary contact (*blue*); a central, so-called 60's helix and loop (*green*); a two-stranded β-sheet connected to the green regions (*yellow*); and two loops (*red* and *white*). (Adapted from SW Englander, L Mayne, and MMG Krishna. *Q Rev Biophys*, 40:287–326, 2007. With permission of Cambridge University Press.)

Whole Secondary Structures Often Fold as a Unit

Proteins tend to fold in units of *motifs* or secondary structures, rather than as individual amino acids. Structural folding units are called *foldons* or *partially unfolded forms*. Foldons have been observed using *hydrogen exchange* (HX). HX can measure either equilibrium fluctuations, or properties of folding kinetics. In equilibrium HX, you have a series of protein solutions with increasing amounts of denaturant. Each amino acid has an amide proton. Prior to the experiment, you replace those amide protons with deuterium atoms. In solution, the deuterium atoms on the protein will exchange with the hydrogen atoms in the surrounding solvent water, with an equilibrium constant that depends on how exposed those amide groups are to the water. It is found that in a series of increasing amounts of denaturant, whole secondary structures are often protonated at once. In kinetic HX, you transiently pulse the conditions so as to capture the protonation state of the protein during a particular time interval of folding. Both experiments show that secondary structures can fold rapidly relative to other folding events. Figure 6.11 shows the sequence of stabilities of the individual structural elements in cytochrome *c*.

Some proteins fold so fast that they appear to have essentially no free-energy barrier. Called *ultrafast folders*, they can fold on timescales of tens of microseconds.

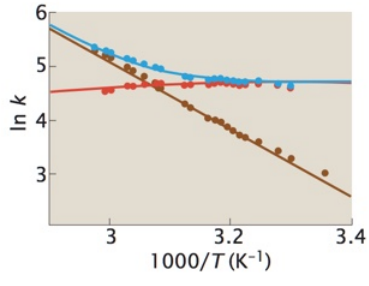

Figure 6.12 Evidence of barrierless folding: folding rate coefficients (*red*) are almost independent of temperature (for the engrailed homeodomain protein). In contrast, unfolding rate coefficients (*brown*) follow normal Arrhenius behavior; see Equation 6.B.12. The observed rate coefficient (*blue*) is the sum of folding and unfolding rates. (Model fits from K Ghosh, SB Ozkan, and KA Dill. *J Am Chem Soc*, 129:11920–11927, 2007. Copyright (2008) National Academy of Sciences, USA.)

Ultrafast Folders Shed Light on the Speed Limits to Protein Folding

How could you determine if a process is barrierless? First, a barrierless process is fast. Second, the absence of a kinetic barrier means you don't have two distinguishable states, so you won't get two-state (single exponential) kinetics. Barrierless processes can have complex kinetics. Third, in a chevron plot for a barrierless folder, you may observe that the folding rate coefficient becomes independent of denaturant concentration at low denaturant. Lowering the denaturant concentration beyond a certain point no longer speeds up folding, because the folding rate is already maximal (see Figure 6.9). And fourth, barrierless processes won't have Arrhenius kinetics. Equation 6.19 describes how two-state folding, which entails a barrier, follows Arrhenius kinetics. When folding has a barrier, higher temperatures lead to faster rates. But when there is no barrier, it means that folding is already happening at the maximum possible rate, so increasing the temperature will not speed it up further. Figure 6.12 shows the case of a protein

for which temperature does not accelerate folding. In ultrafast folders, $k_f(T)$ is approximately constant with temperature. Interestingly, however, the unfolding of ultrafast folders usually does obey Arrhenius kinetics. These temperature dependencies are explained by the Zwanzig–Szabo–Bagchi (ZSB) model (see Appendix 6B).

In the remainder of this chapter, we switch from experiments and macroscopic models to microscopic modeling of how folding processes are encoded in protein structures. The macroscopics aim to capture experimental data in terms of kinetic macrostates, such as N, D, and I_1, I_2, ... Macroscopic modeling is not intended to explain the physical basis of folding, or why one protein folds differently than another, or how the different conditions of solvent or temperature speed up or slow down folding, or to predict folding rates. For the latter questions, we now turn to *microscopic* models of kinetics.

HOW DO PROTEINS FOLD SO FAST? THEY FOLD ON FUNNEL-SHAPED ENERGY LANDSCAPES

Let's return to Levinthal's question: how can proteins fold so quickly? And how are small proteins able to do this, independently of their amino acid sequence, independently of starting denaturing conditions, and no matter what denatured conformation the chain begins in? These questions are answered by recognizing the shape of a protein's *folding energy landscape*. An energy landscape is a mathematical function $G(x_1, x_2, x_3, \ldots, x_L)$ of independent variables $x_1, x_2, x_3, \ldots, x_L$. A protein's independent variables x_i are the chain conformational degrees of freedom, a total of $L = 3n - 6$ of them for a system of n atoms, excluding the six external (three rigid-body translational and three rigid-body rotational) degrees of freedom. These variables may be described in terms of many geometric features, such as bond angles, bond lengths, intermolecular distances, and locations and orientations of water molecules, for example. For protein folding, the function G is the free energy.[3] G is a high-dimensional surface, because it depends on these many degrees of freedom of the protein. What is the nature of this function G? What is the shape of the surface of G as a function of the variables x_i?

Let's consider some possibilities. It could be that a protein's folding energy landscape might have the shape of a golf course in a high-dimensional space (Figure 6.13A). That is, G might be perfectly flat everywhere except for a highly localized well, representing the native structure, where the free energy must be lower than all the other states (since the native state is stable) under native conditions. A golf-course landscape would mean that all conformations of the chain have identical internal free energy, except for the native state, which has a lower internal free energy.

However, statistical mechanical theories developed in the 1980s showed that folding free energy landscapes are not shaped like golf courses. They are shaped like funnels [8, 9, 10]; see Figure 6.13B and

[3] The y-axis on an "energy" landscape is more correctly a free energy, called the *internal free energy*. The internal free energy combines all the energies and entropies, except for the chain conformational entropy. After all, each point on the landscape represents a different chain conformation. The entropies that are included in the internal free energy are those that involve the solvent degrees of freedom.

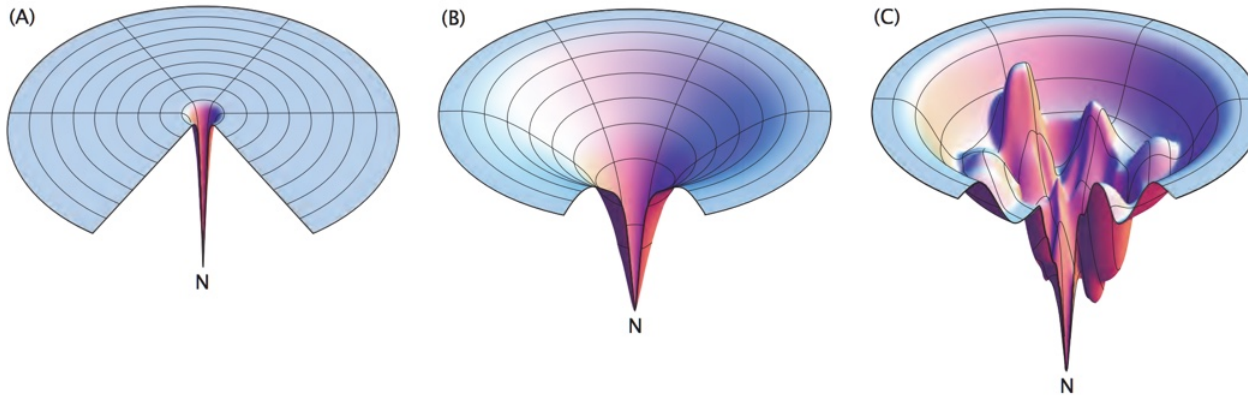

Figure 6.13 Energy landscapes help to visualize protein folding processes. (A) A "golf-course" energy landscape is flat everywhere except for the minimum of the folded state. As in the Levinthal paradox, folding on such a landscape would take a very long time, because the native structure can only be found by random diffusional searching of the entire large conformational space. (B) Protein folding is more appropriately described by a funnel energy landscape, where every random conformational step leading downhill in energy (*y*-axis) also leads to a reduction of the further conformational search, illustrating how protein folding can be so fast. (C) A rugged energy landscape indicates the kinetic traps (local minima) that a typical protein encounters while folding.

Chapter 3. Energy landscapes for folding are large and open at the top and small and confined at the bottom. The funnel shape comes from the statistical mechanical density of states of protein molecules. There are many open chain conformations that, collectively, have a high entropy and few compact native-like states of low free energy. It is easy to see how this rationalizes Levinthal's puzzle. The thermodynamic principle of free-energy minimization means that you can think of the tendency toward equilibrium metaphorically as a ball rolling down a hill. If you roll a ball randomly on the golf landscape, it would take a long time to find a hole on a metaphorical high-dimensional landscape, implying that folding would be very slow. But if you roll a ball randomly on a funnel, even a very high-dimensional one, the ball will roll downhill, finding its way to the bottom, no matter where it starts on the funnel. This indicates both how folding can be so fast and also how the native structure can be reached from any of the huge number of different denatured microstates.

What Do You Learn from Folding Funnels?

First, funnels explain how a solution of protein molecules, all starting from different denatured microstates, can reach the same native structure, and rapidly. Most proteins, irrespective of amino acid sequence, fold on funnel-shaped landscapes because they collapse from the many unfolded states to the one or few native structures. Funnels also explain kinetic heterogeneity, namely that different individual chain conformations reach the native structure through different microscopic folding trajectories, possibly at different rates (Figure 6.14). This folding heterogeneity is at the microstate level, not the macrostate level. To learn about dynamic heterogeneity at this microscopic level, you would need to observe more than just the average folding rate coefficient k_f. You need to measure how much folding flows through different possible microscopic routes. This is becoming possible through single-molecule experiments, which can see individual trajectories of individual molecules. In addition, simple models give a quantitative answer to the Levinthal paradox, of how proteins fold so fast—in milliseconds, rather than millions of years. Appendix 6B describes the ZSB

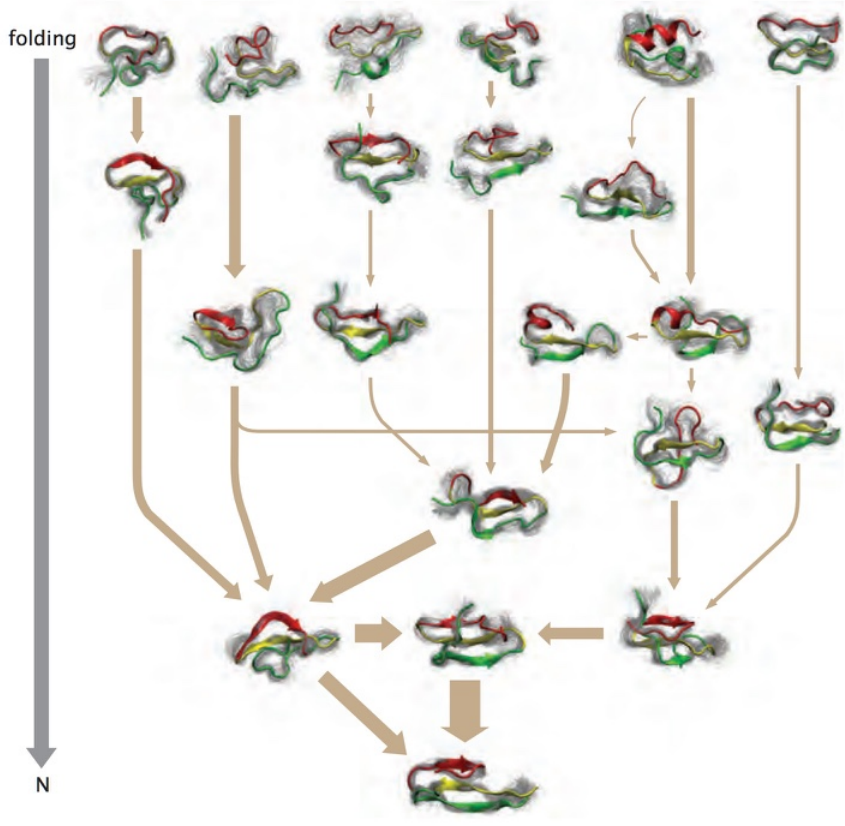

Figure 6.14 Microscopically, the chain folds via many routes. This figure shows a molecular dynamics simulation of the folding of the Pin WW domain. The thickness of the arrows indicates the relative frequencies of the different conformational transitions seen in the simulation. (Adapted from F Noe, C Schutte, E Vanden-Eijnden, et al. *Proc Natl Acad Sci USA*, 106:19011–19016, 2009.)

Model, which shows how protein folding speeds can arise even from quite shallow slopes of folding funnels. Typical protein folding speeds are attained when individual native-like interactions are more favorable than non-native interactions by only 1–2 kcal mol^{-1}.

Another class of models, called *Go models*, which are named after their originator N Go [11], have given useful insights about folding funnels and the folding routes of individual proteins [12, 13]. In a Go model, you assign energetically favorable interactions only to native contacts. In that way, you can turn the true energy landscape into a smooth funnel, to explore the most efficient routes to native states. Another major model is the spin-glass model, which gives a simple approximate way of describing the bumpiness features of folding energy landscapes (see Appendix 6C).

Moreover, cartoons of folding funnels can convey useful insights. For example, Figure 6.13A shows a *golf-course* landscape, illustrating the early expectations of an infinitely slow random search; Figure 6.13B shows a *smooth funnel,* indicating fast folding; Figure 6.13C shows a *bumpy funnel,* indicating small kinetic traps of the type that can reduce folding speeds.

There is experimental evidence for funneled-landscape folding. For example, D Barrick et al. [14] have studied *repeat proteins*, molecules that have multiple units of small foldable peptides. Each repeat unit can fold individually, but their folding rates and equilibria also depend on cooperative interactions among the units. The folding of these proteins occurs through parallel processes because of the many equivalent repeating modular subunits (Figure 6.15).

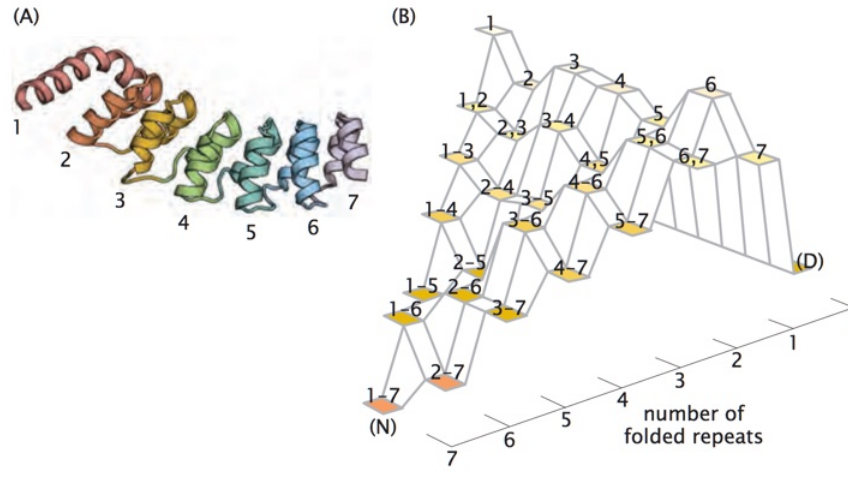

Figure 6.15 A repeating-domain protein lends itself to detailed measurement, showing a funnel-shaped folding landscape. (A) The Notch ankyrin protein has seven repeat units. Folding can be measured in individual domains. (B) The energy landscape of folding states shown as a function of the number of folded repeats and their location. (Adapted from E Kloss, N Courtemanche, and D Barrick. *Arch Biochem Biophys*, 469:83–99, 2008. With permission from Elsevier.)

DIFFERENT PROTEINS CAN FOLD AT VERY DIFFERENT RATES

Protein folding speeds depend not only on mutations, temperature, and denaturants. Protein folding speed also depends on a protein's native structure. How does a protein's sequence and structure encode its folding rate and route? Which conformations are explored and which are not? Is there a general folding mechanism? That is, is there a single narrative for the sequence of structural events that happens that applies across a broad spectrum of different types of proteins? Here, we describe some observations that relate protein structures to folding speeds.

Knowing a protein's native structure can help you predict its folding speed. Figure 6.16 shows how folding speed depends on features of the native structure. Folding speeds vary over orders of magnitude. Figure 6.16A shows that folding rates correlate with the *absolute contact order* (ACO) of native structures, a measure of the "localness" of a protein's native contacts [15]. Proteins having more local contacts and fewer nonlocal contacts in their native structures tend to be faster folders. α-helical proteins tend to fold faster than β-proteins. A similar correlation in Figure 6.16B shows that the more secondary structures a protein has, the slower the protein folds, on average [16]. Why should adding secondary structures slow down the folding process?

The elemental unit of folding kinetics is the foldon. Folding appears to occur by motifs of individual secondary structures. Even though individual secondary structures of a native protein are not stable by themselves, they are more stable than alternative structures and can be further stabilized by assembling together into tertiary structures.

The dominant folding paths form structures in the order *local-first, global-later*. Upon jumping from unfolding to folding conditions, a polymer molecule can only perform localized conformational sampling within small sections of the chain on the earliest timescales—for example, a turn of a helix or a β-strand pair. Forming nonlocal contacts requires larger searches and longer times. On intermediate timescales,

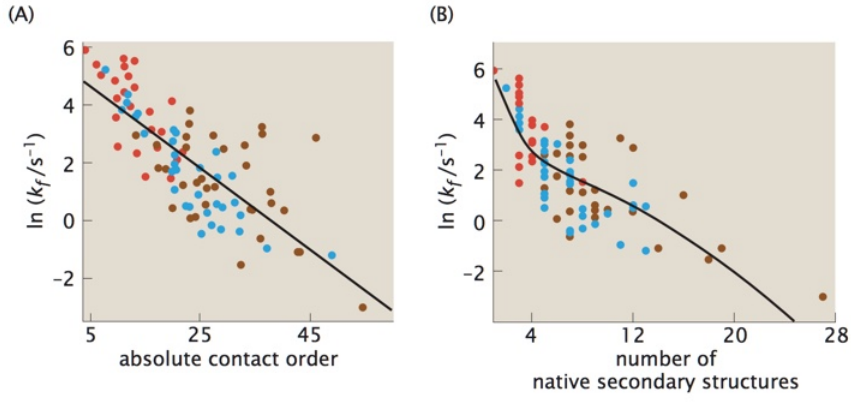

Figure 6.16 Folding rates depend on structural features. (A) Folding rates correlate with the *absolute contact order* (ACO) of a protein's native structure. The ACO measures the average "nonlocalness" of the protein's contacts. Proteins that are mostly helical fold faster, and proteins that are mostly β sheets fold slower. $ACO = (1/C_N)\sum \Delta C_{ij}$, where C_N is the total number of native contacts and $\Delta C_{ij} \equiv |j - i|$ is the *contact order* between residues *i* and *j*, the separation between them along the sequence. (B) Folding rates are slower for proteins having more secondary structures. *Red* shows α-helical proteins, *blue* β-proteins, and *brown* αβ-proteins. (From GC Rollins and KA Dill. *J. Am. Chem. Soc.*, 2014, 136 (32), pp 11420–11427, 2014. Reprinted with permission from American Chemical Society.)

a local piece of chain can *grow* or *zip* into bigger local structures, such as full helices or β-strand pairs. Over the slowest timescales, secondary structure pieces have time to come together and *assemble* into the protein's tertiary structure. Local-first, global-later (also called "Zipping & Assembly" [17]) can rapidly find the native structures of proteins without searching whole conformational spaces [18]. For example, experiments show that inserting polyglycine loops of increasing lengths, which increases the conformational search, also slows the folding process [19].

Figure 6.17 shows a proposed folding mechanism, called the *Foldon Assembly Model* [16]. First, one foldon forms somewhere in the chain. It forms rapidly but in low population. A second foldon then forms by assembling onto the first one. This double-foldon assembly has an even lower population than its predecessor, the single foldon. The process continues, with additional secondary structures assembling onto the growing framework, with diminishing populations (because each helix added is a step uphill in free energy). The final step is the formation of the native structure, which has high population (low free energy), because of additional packing and stabilizing interactions when the protein achieves its native state. Just prior to reaching the native structure, the protein passes through its folding transition state. The landscape is volcano shaped: uphill at first, then downhill at the very end (Figure 6.18).

The Foldon Assembly Model is a general folding mechanism: (i) Secondary structures are not stable alone. (ii) Tertiary interactions help stabilize them. (iii) Two-state proteins have a free-energy barrier between D and N (hence, single-exponential kinetics). (iv) The slowest

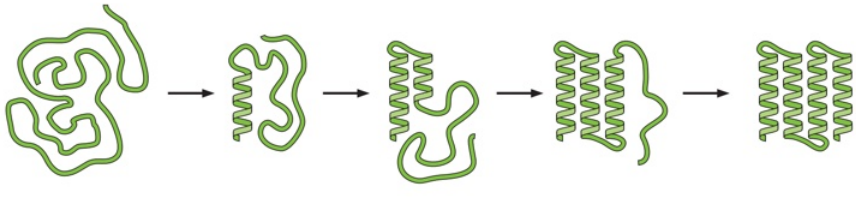

Figure 6.17 Foldon Assembly Model. Under native conditions, a secondary structure flickers on and off—mostly off. But sometimes when it's on, another secondary structure flickers on too, adjacent to the first and stabilized by it. By accretion of secondary structures, the later stages of folding are "less unstable" than the earlier stages, until a fully stable native structure forms at the last step.

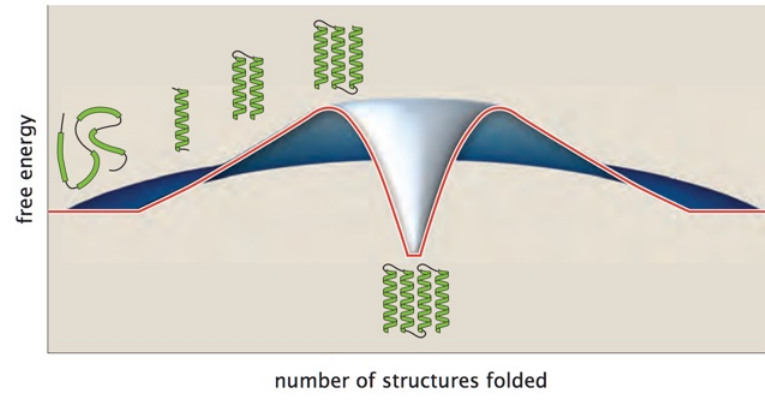

Figure 6.18 The volcano-shaped folding energy landscape shape of the Foldon Assembly Model. Folding is sequential: foldon 1 forms, then foldon 2 adds to it, then foldon 3, etc. These steps are all uphill in free energy, because each individual secondary structure is unfavorable. Only the final step to the full native state is downhill in free energy.

relaxation time should be independent of its starting denatured conformation (see the earlier section in this chapter on chevron plots). The starting state of a protein only affects the fast processes. The slow processes are independent of whether the chain starts from fully denatured or from some other conformation having some residual initial structure. (v) Folding becomes slower with increasing numbers of secondary structures (see Figure 6.16). This model gives a general mechanism, applicable to two-state proteins, over many different folds, and estimates the folding rates from known quantities such as helix–coil and tertiary propensities.

SUMMARY

Measurements of protein folding and unfolding rates give insight into the sequences of folding events and how proteins can fold so quickly, despite the complexities and diversities of their sequences and native structures. Folding rates can depend strongly on temperature, the concentration of denaturants, and on the protein's size, as found on chevron plots, by Φ-value analysis, hydrogen exchange, and other experiments. Small proteins often fold through single-exponential kinetics, while larger proteins often fold through multi-exponential kinetics (involving kinetic intermediates). Master equations provide a general way to capture this phenomenology. Microscopic modeling explains the speed of protein folding in terms of funnel-shaped energy landscapes. The ZSB Model, described in Appendix 6B, shows how a relatively small energy bias (funneling) is sufficient to explain the high speeds of protein folding. In the Foldon Assembly Model, foldons form quickly, then assemble onto an increasingly native structure, for two-state proteins. These simple models give insights into how a protein folds relatively quickly and directly into its native structure.

APPENDIX 6A: MASTER EQUATIONS DESCRIBE DYNAMICS

Master equations are used to describe the time evolution of systems of populations. They treat a very general class of dynamics called *Markov processes,* in which the state of the system at a given time step is fully determined by the state at the previous time step. Master equations resemble classical chemical kinetics, with the fundamental difference that master equations model the probabilistic behaviors of

microscopic states, rather than the deterministic behaviors of average properties, such as concentrations. So, the general approach below can be used to describe macroscopic kinetics, or microscopic stochastics, depending on whether the rate coefficients are found simply by fitting to experimental data (a macroscopic model) or whether they are generated by some underlying physical model of a protein's substructures (a microscopic model). Given a model of n different states (either macroscopic or microscopic), and given the set of arrows and states that constitute the topology of the reaction scheme, you can express the time-dependent populations of the states in terms of a vector

$$\mathbf{P}(t) = \begin{bmatrix} p_1(t) \\ \vdots \\ p_n(t) \end{bmatrix} \tag{6.A.1}$$

and a *rate matrix*

$$\mathbf{W} = \begin{bmatrix} k_{11} & k_{12} & \dots \\ k_{21} & k_{22} & \dots \\ \vdots & \vdots & \ddots \\ k_{n1} & k_{n2} & \dots k_{nn} \end{bmatrix}, \tag{6.A.2}$$

where k_{12} represents the microscopic rate of transition from state 2 to state 1, and the diagonal elements are given by the negative sum of all nondiagonal terms in the same column, that is

$$k_{ii} = -\sum_{j,\, j \neq i} k_{ji}. \tag{6.A.3}$$

As such, the ith diagonal element represents the rate of escape or efflux from state i and all elements in the same row represent the transition/influx into the state i.

The dynamics is described by the set of differential equations:

$$\frac{d\mathbf{P}(t)}{dt} = \mathbf{W}\mathbf{P}(t), \tag{6.A.4}$$

known as the *master equation*. The solution to Equation 6.A.4 can be expressed as

$$\mathbf{P}(t) = e^{\mathbf{W}t}\mathbf{P}(0), \tag{6.A.5}$$

where $\mathbf{P}(0)$ is the initial population, $\mathbf{P}(t)$ at time $t = 0$. How can you evaluate $\exp(\mathbf{W}t)$ and solve Equation 6.A.5? You can do this by first *diagonalizing* the matrix $\mathbf{W}$. Diagonalizing a matrix means that you transform $\mathbf{W}$ to a different matrix $\mathbf{\Lambda}$, in which only the diagonal elements are nonzero:

$$\mathbf{\Lambda} = \begin{bmatrix} \lambda_1 & 0 & 0 & \dots & 0 \\ 0 & \lambda_2 & 0 & \dots & 0 \\ 0 & 0 & \lambda_3 & \dots & 0 \\ \vdots & \vdots & \vdots & \ddots & \vdots \\ 0 & 0 & 0 & \dots & \lambda_n \end{bmatrix}. \tag{6.A.6}$$

The quantities λ_i are called the *eigenvalues*. Note that by definition the rank of the transition matrix is $n-1$, and therefore its eigenvalue decomposition yields $n-1$ nonzero eigenvalues, and one zero eigenvalue (for example, $\lambda_1 = 0$). The remaining eigenvalues are all negative, and their absolute values represent the frequency of different

processes contributing to the overall dynamics. You can perform this transformation by multiplying W by a matrix U:

$$\mathbf{\Lambda} = \mathbf{U}^{-1}\mathbf{W}\mathbf{U}. \tag{6.A.7}$$

Here $\mathbf{U}^{-1}$ is the inverse of U; that is, it satisfies the equation $\mathbf{U}\mathbf{U}^{-1} = \mathbf{U}^{-1}\mathbf{U} = \mathbf{1}$, where 1 is the identity matrix. We show next how to compute the matrices $\mathbf{\Lambda}$ and U. Once you have those matrices, you can compute the full dynamics from

$$\mathbf{P}(t) = \mathbf{U}e^{\mathbf{\Lambda}t}\mathbf{U}^{-1}\mathbf{P}(0). \tag{6.A.8}$$

Note that the product $\mathbf{U}e^{\mathbf{\Lambda}t}\mathbf{U}^{-1}$ represents the time-dependent conditional probability, or transition probability matrix $\mathbf{C}(t)$, the ijth element of which represents the probability of transition from state j to state i at time t. This is a sum of exponentials.[4] You can see this by breaking it into its components:

$$p_i(t) = \sum_k \sum_j U_{ik} e^{-\lambda_k t}[\mathbf{U}^{-1}]_{kj} p_j(0) = \sum_k A_{ik} e^{-\lambda_k t}, \tag{6.A.9}$$

where A_{ik} is the amplitude of the kth relaxation mode of state i and λ_k is the relaxation time of that mode. Note that one relaxation mode has zero eigenvalue (for example, $\lambda_1 = 0$), which, as $t \to \infty$, defines the equilibrium probability of the individual states. That is, the equilibrium probability is found from Equation 6.A.9 upon substituting $t = \infty$, to obtain

$$p_i(\infty) = \sum_j U_{i1}[\mathbf{U}^{-1}]_{1j} p_j(0). \tag{6.A.10}$$

To apply Equation 6.A.8, you must first determine the diagonal matrix $\mathbf{\Lambda}$. Begin with Equation 6.A.7. Multiply it on the left by U to get

$$\mathbf{U}\mathbf{\Lambda} = \mathbf{W}\mathbf{U}. \tag{6.A.11}$$

You can break the matrix U into its vector components:

$$\begin{aligned}\mathbf{U}\mathbf{\Lambda} &= \begin{bmatrix} u_{11} & u_{12} & \cdots \\ u_{21} & u_{22} & \cdots \\ \vdots & \vdots & \ddots \\ u_{n1} & u_{n2} & \cdots \end{bmatrix} \begin{bmatrix} \lambda_1 & 0 & 0 & \cdots & 0 \\ 0 & \lambda_2 & 0 & \cdots & 0 \\ 0 & 0 & \lambda_3 & \cdots & 0 \\ \vdots & \vdots & \vdots & \ddots & \vdots \\ 0 & 0 & 0 & \cdots & \lambda_n \end{bmatrix} \\ &= \begin{bmatrix} \mathbf{u}_1\lambda_1 & \mathbf{u}_2\lambda_2 & \mathbf{u}_3\lambda_3 & \cdots & \mathbf{u}_n\lambda_n \end{bmatrix}\end{aligned} \tag{6.A.12}$$

---

[4] Here is the derivation of Equation 6.A.8 from Equation 6.A.5: the symbolic notation $e^{\mathbf{W}t}$ can be expressed as the series

$$e^{\mathbf{W}t} = \mathbf{1} + \mathbf{W}t + \tfrac{1}{2}\mathbf{W}^2t^2 + \ldots$$

You can express the right-hand side of this equation instead in terms of $\mathbf{\Lambda}$ by transforming each term. Notice that $\mathbf{I} = \mathbf{U}\mathbf{U}^{-1}$ and $\mathbf{W} = \mathbf{U}\mathbf{\Lambda}\mathbf{U}^{-1}$ and $\mathbf{W}^r = \mathbf{U}\mathbf{\Lambda}^r\mathbf{U}^{-1}$ (for any power r, since $\mathbf{\Lambda}$ is a diagonal matrix) so you can express this equation instead as

$$e^{\mathbf{W}t} = \mathbf{U}\left(\mathbf{1} + \mathbf{\Lambda}t + \tfrac{1}{2}\mathbf{\Lambda}^2t^2 + \ldots\right)\mathbf{U}^{-1} = \mathbf{U}e^{\mathbf{\Lambda}t}\mathbf{U}^{-1}.$$

where

$$\mathbf{u}_i = \begin{bmatrix} u_{1i} \\ u_{2i} \\ u_{3i} \\ \vdots \\ u_{ni} \end{bmatrix}.$$

So Equation 6.A.11 becomes

$$\mathbf{u}_j \lambda_j = \mathbf{W}\mathbf{u}_j \tag{6.A.13}$$

Equation 6.A.13 is called an *eigenvalue* equation. To solve it for the values of λ_i, rearrange it into the form

$$(\mathbf{W} - \lambda_j \mathbf{I})\,\mathbf{u}_j = 0. \tag{6.A.14}$$

You can solve this by computing the determinant

$$\det(\mathbf{W} - \lambda_j \mathbf{I}) = 0, \tag{6.A.15}$$

so

$$\det \begin{bmatrix} k_{11} - \lambda_1 & k_{12} & k_{13} & \dots & k_{1n} \\ k_{21} & k_{22} - \lambda_2 & k_{23} & \dots & k_{2n} \\ k_{31} & k_{32} & k_{33} - \lambda_3 & \dots & k_{3n} \\ \vdots & \vdots & \vdots & \ddots & \vdots \\ k_{n1} & k_{n2} & k_{n3} & \dots & k_{nn} - \lambda_n \end{bmatrix} = 0. \tag{6.A.16}$$

Solving this equation gives the eigenvalues λ_i. Once you have the eigenvalues, solve for each $\mathbf{u}$ using Equation 6.A.14 (see the example in Box 6.2). This gives the full dynamical description of a system having a given rate matrix $\mathbf{W}$. Box 6.2 gives a worked example for two-state dynamics. For the more general case of a system consisting of an ensemble of (n) microstates, there are standard computer packages that use this approach to compute eigenvalues and to solve the full dynamics.

Box 6.2 Master Equations Describe Two-State Folding Dynamics

Let's apply the master-equation approach to two-state kinetics for the two states D and N. The master equation is

$$\frac{d\mathbf{P}(t)}{dt} = \mathbf{U}\boldsymbol{\Lambda}\mathbf{U}^{-1}\mathbf{P}(t), \tag{6.A.17}$$

where $\boldsymbol{\Lambda}$ is the diagonal matrix of the eigenvalues of the matrix $\mathbf{W}$ and $\mathbf{U}$ is the matrix of its corresponding eigenvectors. Now, solve for the full time dependence of the populations using $\boldsymbol{\Lambda}$ and $\mathbf{U}$:

$$\mathbf{P}(t) = \mathbf{U}e^{\boldsymbol{\Lambda}t}\mathbf{U}^{-1}\mathbf{P}(0), \tag{6.A.18}$$

where $e^{\boldsymbol{\Lambda}t}$ is a shorthand notation that describes a diagonal matrix composed of the elements $e^{\lambda_i t}$, and λ_i is the ith eigenvalue of $\mathbf{W}$ ($i = 1, 2$ in this case). For two-state dynamics, the rate matrix $\mathbf{W}$ is

$$\mathbf{W} = \begin{bmatrix} -k_f & k_u \\ k_f & -k_u \end{bmatrix}. \tag{6.A.19}$$

Now find the two eigenvalues λ_1 and λ_2 that satisfy the eigenvalue equation

$$\mathbf{W}\mathbf{u}_i = \lambda_i \mathbf{u}_i, \tag{6.A.20}$$

where $\mathbf{u}_i$ is the ith eigenvector ($i = 1, 2$ in the present case). You do this by solving the characteristic equation

$$\det(\mathbf{W} - \lambda\mathbf{I}) = 0, \tag{6.A.21}$$

where $\mathbf{I}$ is the identity matrix of order 2. You can alternatively express this equation in terms of the elements of the matrices:

$$\begin{aligned} &(k_f + \lambda)(k_u + \lambda) - k_u k_f = 0 \\ \Longrightarrow\quad &\lambda^2 + (k_f + k_u)\lambda = 0. \end{aligned} \tag{6.A.22}$$

Solving Equation 6.A.22 gives two values, $\lambda_1 = 0$ and $\lambda_2 = -(k_f + k_u)$, which can be put into a diagonal matrix of eigenvalues,

$$\Lambda = \begin{bmatrix} \lambda_1 & 0 \\ 0 & \lambda_2 \end{bmatrix} = \begin{bmatrix} 0 & 0 \\ 0 & -(k_f + k_u) \end{bmatrix}. \tag{6.A.23}$$

Now, let's determine the eigenvectors. For the eigenvalue corresponding to $\lambda_1 = 0$, the eigenvector is $\mathbf{u}_1 = \begin{bmatrix} u_{11} & u_{21} \end{bmatrix}^T$. Application of Equation 6.A.20 gives

$$\begin{bmatrix} -k_f & k_u \\ k_f & -k_u \end{bmatrix} \begin{bmatrix} u_{11} \\ u_{21} \end{bmatrix} = 0. \tag{6.A.24}$$

Note that these two equations are not independent; that is, you are free to choose one of the components of $\mathbf{u}_1$, and the second is then defined by the relation $k_f u_{11} = k_u u_{21}$. So one possible solution is

$$\mathbf{u}_1 = \begin{bmatrix} k_u \\ k_f \end{bmatrix}. \tag{6.A.25}$$

Similarly for $\lambda_2 = -(k_f + k_u)$, you'll find that the eigenvector is

$$\mathbf{u}_2 = \begin{bmatrix} -1 \\ 1 \end{bmatrix}. \tag{6.A.26}$$

In this case, the two components of u_2 are related by $u_{22} = -u_{21}$. So, we are free to arbitrarily choose $u_{21} = -1$. Now, assemble the eigenvectors into a matrix:

$$\mathbf{U} = \begin{bmatrix} \mathbf{u}_1 & \mathbf{u}_2 \end{bmatrix} = \begin{bmatrix} k_u & -1 \\ k_f & 1 \end{bmatrix}. \tag{6.A.27}$$

We also need the inverse of $\mathbf{U}$, which is obtained by solving $\mathbf{U}^{-1}\mathbf{U} = 1$. The result is

$$\mathbf{U}^{-1} = \frac{1}{k_u + k_f} \begin{bmatrix} 1 & 1 \\ -k_f & k_u \end{bmatrix}. \tag{6.A.28}$$

Finally, to obtain the time-dependent populations $\mathbf{P}(t)$, insert $\boldsymbol{\Lambda}$ (Equation 6.A.23), $\mathbf{U}$ (Equation 6.A.27), and $\mathbf{U}^{-1}$ (Equation 6.A.28) into Equation 6.A.18, to get

$$\begin{bmatrix} P_D(t) \\ P_N(t) \end{bmatrix} = \begin{bmatrix} k_u & -1 \\ k_f & 1 \end{bmatrix} \begin{bmatrix} 0 & 0 \\ 0 & e^{-(k_u + k_f)t} \end{bmatrix} \begin{bmatrix} \frac{1}{k_u + k_f} & \frac{1}{k_u + k_f} \\ -\frac{k_f}{k_u + k_f} & \frac{k_u}{k_u + k_f} \end{bmatrix} \begin{bmatrix} P_D(0) \\ P_N(0) \end{bmatrix}. \tag{6.A.29}$$

Performing these matrix multiplications gives $P_D(t)$ and $P_N(t)$. This is Equation 6.7 in the main text.

APPENDIX 6B: THE ZWANZIG–SZABO–BAGCHI MODEL SHOWS HOW FUNNELS ACCELERATE FOLDING

How does a funnel-shaped landscape explain fast folding? To explore this, let's express a protein's folding equilibrium and kinetics in a highly simplified way. Represent a chain of L amino acids as a one-dimensional string of symbols

nnndddnnnnnnddddn...,

where each n indicates that a particular residue is in its folded native-like conformation, and each d indicates that a particular residue is in an unfolded non-native conformation. This resembles the way we treated the helix–coil transition in Chapter 5.

Here, we describe the Zwanzig–Szabo–Bagchi (ZSB) model, which shows how Levinthal's paradox is resolved by energy funneling [20, 21]. Let $m = 1, 2, 3, \ldots L$ represent the number of "mistakes" d (that is, native contacts not yet made) in the string. So, $m = 0$ represents the folded native state; $m = 1$ means the molecule has all n's except for one d somewhere in the string; and $m = L$ means that the molecule has no correct (that is, folded native) pieces of structure. m represents a simple one-dimensional "reaction coordinate" for folding.

Now, let's model the energies of a funnel landscape. The larger the number of mistakes in a given conformation, the higher is the energy of that conformation. To keep the model simple, we first suppose that the energy $U(m)$ is a linear function of the number of mistakes, $U(m) = m\epsilon$, where $\epsilon > 0$ is the energy cost of each mistake. Figure 6.B.1 is the energy landscape of the ZSB Model.

However, we need one more ingredient for the ZSB Model. To capture the two-state nature of folding equilibria, we also need an *energy gap*. We assume that the native state is further stabilized by an energy $\epsilon_0 > 0$. Figure 6.B.1 shows this linear energy funnel plus native well.

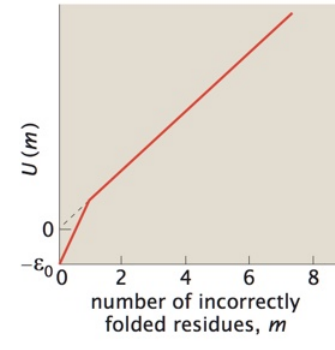

Figure 6.B.1 ZSB funnel energy landscape. In the ZSB Model, the energy increases linearly with m, the number of non-native contacts ("mistakes"). Each mistake costs an energy ϵ. The step from $m = 0$ (native) to $m = 1$ is steeper, with slope ϵ_0. This defines the funnel shape of this landscape, projected onto a one-dimensional axis of m.

The Equilibrium Properties of the ZSB Funnel Landscape Model

Before looking at the folding kinetics, let's consider the equilibrium predictions of the ZSB Model. The equilibrium probability $P_m(\text{eq})$ that a chain has m mistakes is given by

$$P_m(\text{eq}) = \frac{L!}{m!(L-m)!} K^m Q^{-1}, \tag{6.B.1}$$

where K is the Boltzmann factor,

$$K = (z-1)e^{-\beta\epsilon}. \tag{6.B.2}$$

K is an equilibrium constant per residue that gives the energetic disadvantage ϵ and the entropic advantage $z - 1$ of converting each residue from n to d. z is the total number of rotational isomers, so $z - 1$ is the number of isomers in wrong states, and $\beta = (RT)^{-1}$. The combinatorial factor in Equation 6.B.1 counts the number of ways you can arrange m d's and $(L - m)$ n's in a one-dimensional string. Q is the partition

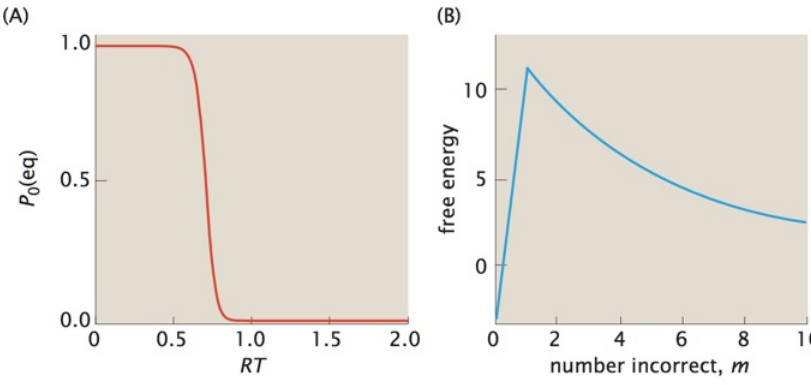

Figure 6.B.2 The ZSB Model predicts two equilibrium states in protein folding. (A) The plot of the native population versus temperature is sigmoidal, indicating cooperativity. (B) There are two minima in the energy versus the number of mistakes, m, corresponding to the native state ($m = 0$) and a denatured state where approximately half of the amino acids are unfolded or misfolded.

function, the sum over the statistical weights of all the states:[5]

$$Q = e^{\beta\epsilon_0} + \sum_{m=1}^{L} \left(\frac{L!}{m!(L-m)!} K^m \right) = e^{\beta\epsilon_0} + (1+K)^L - 1. \qquad (6.B.3)$$

The binomial expression $(1 + K)^L$ would account for all the possible states of the system if the native state were defined as the state of zero energy. However, our model defines an additional stabilization for the native state, to represent the high level of cooperativity observed in two-state proteins. The term $e^{\beta\epsilon_0} - 1$ subtracts the term from the series for $m = 1$ and adds an additional term to give the corrected weight of the extra-stabilized native state.

The equilibrium populations of the native (folded) state ($m = 0$, here called P_N rather than P_0) and the *first excited* state ($m = 1$) are

$$P_N(\text{eq}) = \frac{e^{\beta\epsilon_0}}{Q} \quad \text{and} \quad P_1(\text{eq}) = \frac{LK}{Q}. \qquad (6.B.4)$$

Figure 6.B.2A shows that the native (folded) state population P_0 (see Equation 6.B.4) undergoes a sharp transition with temperature. Thus, the ZSB Model predicts that folding involves a two-state equilibrium. You can see this from the free energy $G_m = -RT \ln P_m(\text{eq})$ as a function of the *order parameter* m. Figure 6.B.2B gives the free energy calculated by substituting $P_m(\text{eq})$ from Equation 6.B.1, and shows that the model predicts two stable states, denatured and native, with a barrier in between (that is, the definition of two-state equilibrium).

The ZSB Model Relates Landscape Shape to Folding Speed

Now, let's compute the folding and unfolding kinetics given by the ZSB Model. Express the kinetics in terms of a master equation

$$\frac{dP_N(t)}{dt} = k_0 P_1(t) - k_1 P_N(t), \qquad (6.B.5)$$

where $P_N(t)$ is the native population as a function of time, $P_1(t)$ is the population of the first-excited state, k_0 is the rate coefficient for the folding transition to the native state from the first-excited state ($1 \rightarrow$

[5] The last equality in Equation 6.B.3 follows from the binomial relation $(x+y)^L = \sum_{m=0}^{L} \{L!/[m!(L-m)!]\} x^{L-m} y^m$, where $x = 1$ and $y = K$.

N), and k_1 is the rate coefficient for the unfolding (N $\rightarrow$ 1). We want to obtain the folding and unfolding rate coefficients k_f and k_u, so we want to convert Equation 6.B.5 into the two-state form

$$\frac{dP_{\mathrm{N}}}{dt} = k_f P_{\mathrm{D}}(t) - k_u P_{\mathrm{N}}(t). \tag{6.B.6}$$

To solve this equation, we first express k_1 in terms of k_0, a given rate coefficient. The principle of detailed balance applied to Equation 6.B.5 asserts that at equilibrium we must have $k_0 P_1(\mathrm{eq}) = k_1 P_{\mathrm{N}}(\mathrm{eq})$. Combining this with Equation 6.B.4 gives

$$k_1 = k_0 \frac{P_1(\mathrm{eq})}{P_{\mathrm{N}}(\mathrm{eq})} = k_0 LK e^{-\beta\epsilon_0}. \tag{6.B.7}$$

Second, express $P_1(t)$ in terms of $P_{\mathrm{N}}(t)$. We assume that the system is in rapid equilibrium among all unfolded denatured states ($m = 1, 2, 3, \ldots, L$). So, we take the time-dependent population of state 1 to be proportional to the time-dependent population of the set of denatured states (D) ($m > 0$):

$$\begin{aligned} \frac{P_1(t)}{P_{\mathrm{D}}(t)} &= \frac{LK/Q}{Q_{\mathrm{D}}/Q} \\ \Rightarrow P_1(t) &= \frac{LK}{Q_{\mathrm{D}}}[1 - P_{\mathrm{N}}(t)], \end{aligned} \tag{6.B.8}$$

where $Q_{\mathrm{D}} = (1+K)^L - 1$ is the partition function for the denatured state (that is, the full partition function excluding the extra native term) given by Equation 6.B.3. We have also used $P_{\mathrm{D}}(t) = 1 - P_{\mathrm{N}}(t)$. Now, substitute Equations 6.B.8 and 6.B.7 into Equation 6.B.5 to get

$$\begin{aligned} \frac{dP_{\mathrm{N}}}{dt} &= k_0 LK \left[\frac{1}{Q_{\mathrm{D}}} P_{\mathrm{D}}(t) - e^{-\beta\epsilon_0} P_{\mathrm{N}}(t) \right] \\ &= \left(\frac{k_0 LK}{Q_{\mathrm{D}}} \right) P_{\mathrm{D}}(t) - \left(k_0 LK e^{-\beta\epsilon_0} \right) P_{\mathrm{N}}(t). \end{aligned} \tag{6.B.9}$$

Comparison with Equation 6.B.6 shows that $k_f = k_0 LK/Q_{\mathrm{D}}$ and $k_u = k_0 LK\, e^{-\beta\epsilon_0}$. In Boxes 6.3 and 6.4, we compute the folding times on a golf course and funnel landscape, respectively.

Box 6.3 Folding on a Golf-Course Landscape Would Be Very Slow

How fast would proteins fold if their energy landscapes were flat, shaped like a golf course? Suppose you have a protein of $L = 100$ amino acids. Let's take $k_0 = 10^{-6}$ s (see page 135) and $z = 4$, which are reasonable estimates. For a flat energy landscape, you have a slope $\epsilon = 0$ and $K = z - 1$ (see Equation 6.B.2). So, $Q_{\mathrm{D}} = z^L - 1 \approx z^L$. Then, Equation 6.B.13 gives the folding time as

$$\begin{aligned} \tau_f &= \frac{z^L}{k_0 L(z-1)} \\ &= \frac{4^{100}}{(10^6\ \mathrm{s}^{-1})(100)(3)} \approx 5 \times 10^{51}\ \mathrm{s}, \end{aligned} \tag{6.B.10}$$

which is astronomically large. If proteins were to fold on golf-course energy landscapes, it would take figuratively "forever."

Box 6.4 Folding on a Smooth Funnel Landscape Is Fast

Figure 6.B.3 shows that even small biases of energy toward the native state can speed up folding enormously. Suppose the energy advantage of forming a native contact is just $\epsilon = 2\,\text{kcal mol}^{-1}$ ($3.34RT$). For $z = 4$ and $L = 100$, this gives $K = (z-1)e^{-\beta\epsilon} = 0.106$, so $Q_D = (1+K)^L - 1 \approx 2.4 \times 10^4$. Then

$$\tau_f = \frac{Q_D}{k_0 LK} = \frac{2.4 \times 10^4}{(10^6\,\text{s}^{-1})(100)(0.106)} \approx 2.3 \times 10^{-3}\,\text{s}. \qquad (6.B.11)$$

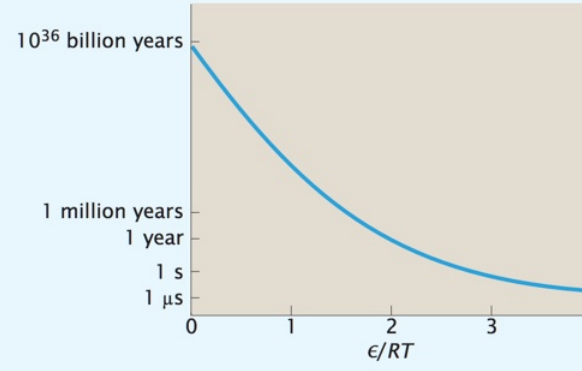

Figure 6.B.3 The time required for a protein to fold depends on its energy bias, ϵ/RT. This shows how a protein can fold rapidly, in fractions of a second, because of the funnel shape of its energy landscape, even if the energy bias is relatively small, $\epsilon \approx 2RT$. (Adapted from R Zwanzig, A Szabo, and B Bagchi. *Proc Natl Acad Sci USA*, 89:20–22, 1992.)

Comparing this folding time of 2 ms with that in Box 6.3, you see that funneling accelerates folding by more than 50 orders of magnitude, given only a bias of $-2\,\text{kcal mol}^{-1}$ when residues are in native-like versus non-native-like conformations. Figure 6.B.3 shows that the predicted folding speed has a strong dependence on the slope of the energy landscape.

The ZSB Model Explains the Unusual Temperature Dependences of Ultrafast Folders

Recall from Figure 6.12 that the folding rates of ultrafast folders cannot be increased by temperature; they are already folding at maximum speed. However, the *unfolding* kinetics of ultrafast folders often follows Arrhenius kinetics (see Figure 6.12). The ZSB Model explains both features. First, the temperature independence of $k_f(T)$ comes from a balance of two quantities, $K(T)$ and $Q_D(T)$, in Equation 6.B.11. Second, it also explains the Arrhenius kinetics of unfolding. Substitute the definition of $K(T)$ from Equation 6.B.2 into $k_u = k_0 LK(T)e^{-\beta\epsilon_0}$ deduced from Equation 6.B.9, and take the logarithm to get

$$\ln k_u(T) = \text{constant} - \frac{\epsilon + \epsilon_0}{RT}, \qquad (6.B.12)$$

which is the Arrhenius law (if ϵ and ϵ_0 are constants, as we have assumed), consistent with experiments (see Figure 6.12).

Equation 6.B.9 with Equation 6.B.6 shows that the folding rate coefficient k_f, or its inverse, the folding time τ_f, is

$$k_f = \frac{1}{\tau_f} = \frac{k_0 LK}{Q_D}, \tag{6.B.13}$$

as given in the main text. And the unfolding rate coefficient is

$$k_u = k_0 LK e^{-\beta \epsilon_0}. \tag{6.B.14}$$

The Foldon Assembly Model is a Folding Mechanism Variant of the ZSB Model

The Foldon Assembly Model is a variant of the ZSB Model; for details, see [16]. But, in short, here is how the Foldon Assembly Model differs from the ZSB Model, Equation 6.B.9, for the specific example of a four-helix-bundle protein. The native population is $P_N(t)$, and

$$\frac{dP_N}{dt} = \left(\frac{4k_0 K_2^3 K_3^3}{Q_D}\right) P_D(t) - \left(\frac{4k_0 K_2^3 K_3^3}{Q_N}\right) P_N(t). \tag{6.B.15}$$

From Equation 6.B.15, we get the rate coefficient for forming the native structure as $4k_0 K_2^3 K_3^3 Q_D$. The factor of 4 accounts for the combinatorics that any one of the four helices can form first. k_0 is the intrinsic rate coefficient for forming a helix. The factor K_2^3 is the equilibrium coefficient for forming the three helices of the precursor to the native state, as if they were independent. However, the helices are not independent. Their interaction is treated by the factor of K_3^3, which accounts for the pairwise tertiary interactions among the helices (hence the subscript 3). Each helix is surrounded by three other helices, each of which stabilizes the first by a factor $K_3 > 1$.

APPENDIX 6C: PROTEIN FOLDING FUNNELS CAN BE BUMPY: THE SPIN-GLASS MODEL

Spin-glass models, adapted from the physics of glassy materials to proteins by PG Wolynes, JN Onuchic, Z Luthy-Schulten, EI Shakhnovich, D Thirumalai, and others, capture essential aspects of the bumpiness of protein folding funnels [22]. Consider a probability distribution $p(U)$ of the protein chain conformations as a function of their energy U. U is the *internal free energy*, the sum of all the intermolecular interactions, due to hydrogen bonding, charge and steric interactions, and hydrophobic and solvation interactions, of a single given chain conformation. We are interested in how the chain entropy $S(U)$, representing how many chain conformations have that energy, depends on U. Focus on the most highly populated denatured state, for which the ensemble-average energy is $\langle U \rangle$. Assume that the distribution around that most-probable denatured state is Gaussian (Figure 6.C.1):

$$p(U) = \frac{1}{\sqrt{2\pi\delta_U^2}} e^{-(U-\langle U \rangle)^2/2\delta_U^2}. \tag{6.C.1}$$

where δ_U^2 is the variance of the energy fluctuations (so δ_U has units of energy and is the standard deviation), representing the width of the Gaussian distribution and characterizing the bumpiness of the landscape for a given protein or foldamer.

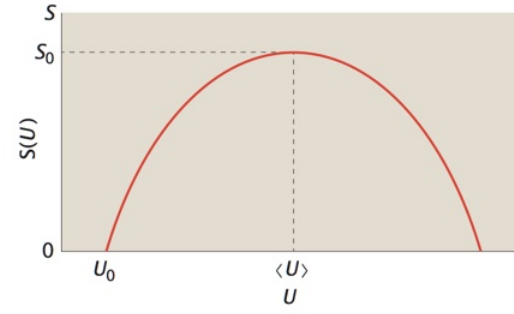

Figure 6.C.1 The Gaussian energy distribution of the spin-glass model. The entropy $S(U)$ is a parabolic function of energy U. This surface is characterized by two slopes, which are inverses of the glass temperature T_g (a measure of bumpiness) and the denaturation temperature T_f (a measure of protein stability).

Substitute $p(U)$ from Equation 6.C.1 into the Boltzmann distribution expression $S(U) = S_0 + k \ln p(U)$, to get

$$S(U) = S_0 + \frac{k(U - \langle U \rangle)^2}{2\delta_U^2}, \tag{6.C.2}$$

where S_0 is the entropy of the dominant denatured state. The central idea of this model is that proteins have *glass-like* states. In a glass, as the system moves to lower and lower energies, it reaches a *kinetic trap*, that is, a lowest possible energy U_0, at which there is only a single microstate, so the entropy of that state is zero: $S(U_0) = 0$. This is called the *entropy catastrophe*. The system cannot easily reach even lower energies, to achieve the global minimum in energy, the crystalline state. Applied here to proteins, the idea is that a folding protein can get caught in a kinetic trap, resembling a glassy state, which slows its folding progress toward its native state. The native state has global minimum energy U_N, but the kinetic trap energy is higher, $U_0 > U_N$. Our aim is to compute the temperature of the entropy catastrophe, T_g, called the *glass transition temperature*.

To find the energy, $U = U_0$, of the entropy catastrophe trap, substitute $S(U_0) = 0$ into Equation 6.C.2 to get

$$\langle U \rangle - U_0 = \delta_U \sqrt{\frac{2S_0}{k}}. \tag{6.C.3}$$

(We have taken only the positive root because our interest is in the left side of the $S(U)$ curve, $T_g > 0$.) Now, thermodynamics gives a fundamental relationship [23] for computing the temperature if you know the function $S(U)$:

$$\frac{1}{T_g} = \left.\frac{\partial S}{\partial U}\right|_{U_0} = \frac{k(U_0 - \langle U \rangle)}{\delta_U^2}, \tag{6.C.4}$$

where we have evaluated this function at the glass point $U = U_0$. Finally, for comparison, the folding temperature occurs where $T_f \approx \Delta U / S_0$, where $\Delta U = \langle U \rangle - U_N$, so we can compute a dimensionless ratio

$$\frac{T_f}{T_g} = \frac{\Delta U}{\delta_U} \sqrt{\frac{2k}{S_0}} \approx \frac{\Delta U}{N \delta_U}. \tag{6.C.5}$$

In the last step, we have approximated the denatured state entropy as $S_0 = k \ln z^N$, where z is the number of rotamers per backbone bond and N is the number of chain bonds, and we have left out constants of order unity.

The main points that emerge from such spin-glass models are that (1) proteins can have glass-like kinetic traps that slow the progress of folding; (2) the bumpiness of an energy landscape can be approximated as δ_U, a standard deviation of a Gaussian function; (3) kT_g defines an energy scale for fluctuations, which is of order δ_U/N; and (4) T_f/T_g is a useful dimensionless quantity for comparing polymer folding speeds (T_f/T_g is smaller for slower-folding molecules.)

REFERENCES

[1] C Levinthal. Are there pathways for protein folding? *J Chim Phys PCB*, 65:44–45, 1968.

[2] SJ Hagen, J Hofrichter, A Szabo, and WA Eaton. Diffusion-limited contact formation in unfolded cytochrome *c*: estimating the maximum rate of protein folding. *Proc Natl Acad Sci USA*, 93:11615–11617, 1996.

[3] PS Kim and RL Baldwin. Structural intermediates trapped during the folding of ribonuclease A by amide proton exchange. *Biochemistry*, 19:6124–6129, 1980.

[4] SB Ozkan, KA Dill, and I Bahar. Computing the transition state populations in simple protein models. *Biopolymers*, 68:35–46, 2003.

[5] CM Dobson, PA Evans, and SE Radford. Understanding how proteins fold: the lysozyme story so far. *Trends Biochem Sci*, 19:31–37, 1994.

[6] AR Fersht, A Matouschek, and L Serrano. The folding of an enzyme. I. theory of protein engineering analysis of stability and pathway of protein folding. *J Mol Biol*, 224:771–784, 1992.

[7] KL Maxwell, D Wildes, A Zarrine-Afsar, et al. Protein folding: defining a "standard" set of experimental conditions and a preliminary kinetic data set of two-state proteins. *Protein Sci*, 14:602–616, 2005.

[8] KA Dill. Theory for the folding and stability of globular proteins. *Biochemistry*, 24:1501, 1985.

[9] JD Bryngelson and PG Wolynes. Spin glasses and the statistical mechanics of protein folding. *Proc Natl Acad Sci USA*, 84:7524–7528, 1987.

[10] PE Leopold, M Montal, and JN Onuchic. Protein folding funnels: A kinetic approach to the sequence–structure relationship. *Proc Natl Acad Sci USA*, 89:8721–8725, 1992.

[11] N Go. Theoretical studies of protein folding. *Annu Rev Biophys Bioeng*, 12:183, 1983.

[12] V Muñoz and WA Eaton. A simple model for calculating the kinetics of protein folding from three-dimensional structures. *Proc Natl Acad Sci USA*, 96:11311–11316, 1999.

[13] PC Whitford, JK Noel, S Gosavi, et al. An all-atom structure-based potential for proteins: Bridging minimal models with all-atom empirical forcefields. *Proteins*, 75:430–441, 2009.

[14] E Kloss, N Courtemanche, and D Barrick. Repeat-protein folding: New insights into origins of cooperativity, stability, and topology. *Arch Biochem Biophys*, 469:83–99, 2008.

[15] KW Plaxco, KT Simons, and D Baker. Contact order, transition state placement and the refolding rates of single domain proteins. *J Mol Biol*, 277:985–994, 1998.

[16] GC Rollins and KA Dill. General mechanism of two-state protein folding kinetics. *J Am Chem Soc*, 136:11420–11427, 2014.

[17] SB Ozkan, GA Wu, JD Chodera, and KA Dill. Protein folding by zipping and assembly. *Proc Natl Acad Sci USA*, 104:11987–11992, 2007.

[18] VA Voelz and KA Dill. Exploring zipping and assembly as a protein folding principle. *Proteins*, 66:877–888, 2007.

[19] AR Viguera and L Serrano. Loop length, intramolecular diffusion and protein folding. *Nat Struct Biol*, 4:939–946, 1997.

[20] R Zwanzig, A Szabo, and B Bagchi. Levinthal's paradox. *Proc Natl Acad Sci USA*, 89:20–22, 1992.

[21] R Zwanzig. Simple model of protein folding kinetics. *Proc Natl Acad Sci USA*, 92:9801–9804, 1995.

[22] JN Onuchic, Z Luthey-Schulten, and PG Wolynes. Theory of protein folding: The energy landscape perspective. *Annu. Rev. Phys. Chem.*, 48:545–600, 1997.

[23] KA Dill and S Bromberg. *Molecular Driving Forces: Statistical Thermodynamics in Biology, Chemistry, Physics and Nanoscience, 2nd ed.* Garland Science, New York, 2011.

SUGGESTED READING

Fersht A, *Structure and Mechanism in Protein Science: A Guide to Enzyme Catalysis and Protein Folding*. WH Freeman, New York, 1998.

Gruebele M, Dave K, and Sukenik S, Globular Protein folding *in vitro* and *in vivo*. *Annu Rev Biophys*, 45:233–251, 2016.